AMERICAN SOCIETY FOR MICROBIOLOGY | Applied and Environmental Microbiology

High-Throughput Single-Cell Cultivation on Microfluidic Streak Plates

Cheng-Ying Jiang,[a] Libing Dong,[b] Jian-Kang Zhao,[a] Xiaofang Hu,[b] Chaohua Shen,[a] Yuxin Qiao,[a] Xinyue Zhang,[b] Yapei Wang,[b] Rustem F. Ismagilov,[c] Shuang-Jiang Liu,[a] Wenbin Du[a]

State Key Laboratory of Microbial Resources, Institute of Microbiology, Chinese Academy of Sciences, Beijing, China[a]; Department of Chemistry, Renmin University of China, Beijing, China[b]; Division of Chemistry and Chemical Engineering, California Institute of Technology, Pasadena, California, USA[c]

This paper describes the microfluidic streak plate (MSP), a facile method for high-throughput microbial cell separation and cultivation in nanoliter sessile droplets. The MSP method builds upon the conventional streak plate technique by using microfluidic devices to generate nanoliter droplets that can be streaked manually or robotically onto petri dishes prefilled with carrier oil for cultivation of single cells. In addition, chemical gradients could be encoded in the droplet array for comprehensive dose-response analysis. The MSP method was validated by using single-cell isolation of *Escherichia coli* and antimicrobial susceptibility testing of *Pseudomonas aeruginosa* PAO1. The robustness of the MSP work flow was demonstrated by cultivating a soil community that degrades polycyclic aromatic hydrocarbons. Cultivation in droplets enabled detection of the richest species diversity with better coverage of rare species. Moreover, isolation and cultivation of bacterial strains by MSP led to the discovery of several species with high degradation efficiency, including four *Mycobacterium* isolates and a previously unknown fluoranthene-degrading *Blastococcus* species.

Microbial communities function in natural and artificial environments such as soil (1), the human gut (2), and wastewater treatment facilities (3). Analyses of these communities indicate that they are composed of abundant and rare biospheres (4). The abundant biosphere may account for a large portion of a microbial biomass in terms of individual populations, while the rare biosphere can comprise up to 75% of the total biomass, although each rare species may represent less than 0.1% of the biomass (5, 6). Both abundant and rare microorganisms are considered to play important roles in maintaining the structure and function of communities, and their metabolisms shape the physiochemical dimensions of their environments (5). Microbial populations in environments are both numerous and diverse; e.g., a single gram of soil may contain $>2 \times 10^9$ microbes, representing 2,000 to 18,000 species (1). Thus, unraveling the structure and composition of microbial communities in environments is challenging. For example, members of the rare biosphere can be easily overlooked or masked when communities are cultivated by traditional methods (e.g., petri dish agar or nutrient broth) because of their low cell densities, low rates of growth, or resistance to cultivation (7–9). Even with culture-independent molecular methods such as metagenomics or high-throughput sequencing tools, the rare biosphere is not adequately represented (10, 11).

Numerous efforts have been made to face these challenges and to unravel the unexplored diversity of microbial species (12, 13). Culture-independent molecular tools are being improved by more powerful metagenomic technologies and bioinformatic approaches (14), as well as single-cell sequencing (15). However, axenic cultures are indispensable for advancing the true understanding of microorganisms, as well as their functions in environments. The majority of microbial isolates are obtained by plating on agar, the standard technique since 1882. On a conventional agar plate, the number of microbial colonies per plate is limited to a few hundred. An important factor that contributes to this limitation is that abundant and fast-growing microbes compete for space and mask or inhibit the growth of rare or slow-growing species. Recently, culture-dependent methods have been improved considerably by the use of oligotrophic media (16), media that mimic natural conditions (17, 18), and diffusive growth compartments (19–21). These innovations have led to the cultivation of novel microbes that had been overlooked or considered to be recalcitrant when current techniques are used. Considering that 85 to 99% of microbes are considered "uncultivable" (13), challenges in unraveling microbial diversity remain.

Droplets surrounded by immersion oil have been used for observation of motility and growth of single bacterial cells since 1954 (22). In recent years, droplet microfluidics has attracted substantial interest because of the capacity for high-throughput screening and single-cell sorting (23). Great efforts have been dedicated to microbial cultivation by developing large-scale storage of droplets in microchannels (24, 25) or microfabricated chambers (26–28). Compared with diffusive compartments, isolation in droplets offers advantages, including prevention of interspecific competition and elimination of biases due to differences in growth rates (29), and is more likely to recover species for scale-up with well-defined cultivation conditions. Recently, splitting of individual microcultures with a SlipChip device has enabled PCR identification of target species even under conditions of high background noise (i.e., interfering species) and resulted in the isolation of a previously uncultivated gut bacterium (26). However, further development is needed to effectively cultivate encapsulated cells over pro-

Received 4 November 2015 **Accepted** 19 January 2016

Accepted manuscript posted online 5 February 2016

Citation Jiang C-Y, Dong L, Zhao J-K, Hu X, Shen C, Qiao Y, Zhang X, Wang Y, Ismagilov RF, Liu S-J, Du W. 2016. High-throughput single-cell cultivation on microfluidic streak plates. Appl Environ Microbiol 82:2210–2218. doi:10.1128/AEM.03588-15.

Editor: R. E. Parales, University of California—Davis

Address correspondence to Wenbin Du, wenbin@im.ac.cn, or Shuang-Jiang Liu, liusj@im.ac.cn.

C.-Y.J., L.D., and J.-K.Z. contributed equally to this work.

Supplemental material for this article may be found at http://dx.doi.org/10.1128/AEM.03588-15.

longed time periods and to be able to access specific droplets containing targeted species at multiple time points. More importantly, the proficiency of droplets in revealing microbial diversity at the community level has not yet been fully demonstrated.

Here, we introduce the microfluidic streak plate (MSP) technique, which enables the growth of tens of thousands of microcultures in disposable petri dishes. We apply the MSP method to explore microbial diversity in, as well as isolate and cultivate single bacterial cells from, a soil community that was enriched with polycyclic aromatic hydrocarbons (PAH). A previously unknown fluoranthene-degrading *Blastococcus* isolate that belongs to the rare species was obtained by this MSP method.

MATERIALS AND METHODS

Chemicals and materials. All solvents and chemicals purchased from commercial sources were used as received unless otherwise stated. Mineral oil was purchased from J&K Scientific (Beijing, China). Silicone oil (10 centistokes viscosity) was purchased from Wacker Chemie AG (Munich, Germany). Fluoranthene was purchased from Sigma-Aldrich (St. Louis, MO). 2,5-Dihydroxybenzoic acid (DHB) was purchased from Merck (Hohenbrunn, Germany). Food dye pigments were purchased from Duofuyuan (Tianjin, China). Dichlorodimethylsilane and 3-aminopropyl triethoxysilane (APTES) were purchased from Alfa Aesar (Tianjin, China). Silicon wafers were purchased from Qimin Silicon Material Co., Ltd. (Shanghai, China). Photomasks were designed in AutoCAD and ordered from MicroCAD Photomask Co., Ltd. (Shenzhen, China). SU-8 photoresist was purchased from MicroChem Corp. (Newton, MA). Polydimethylsiloxane (PDMS) was purchased from Momentive Performance Materials Inc. (Waterford, NY). Fused-silica capillaries were purchased from Polymicro (Phoenix, AZ). Teflon tubing was purchased from Zeus (Orangeburg, SC). Gastight glass syringes were purchased from Agilent (Palo Alto, CA). Polystyrene (PS) petri dishes (90 mm in diameter) and Axygen pipette tips were purchased from Corning (Tewksbury, MA).

Equipment and software. PicoPlus Elite syringe pumps were purchased from Harvard Apparatus (Holliston, MA). Programs for controlling syringe pumps and the automated dish drive were written in LabVIEW (National Instruments, Austin, TX). Droplets were imaged by a Ti-Eclipse inverted fluorescence microscope (Nikon, Tokyo, Japan) equipped with a CoolSNAP HQ^2 charge-coupled device camera (Photometrics, Tucson, AZ) and with fluorescein isothiocyanate (FITC; excitation, 480/40 nm; emission, 527/30 nm) and G-2A (excitation, 535/50 nm; emission, 590 nm long-pass) filter cubes. Micrographs were collected and analyzed by NIS-Elements Advanced Research software (Nikon, Tokyo, Japan). An Epson L551 Inkjet printer (Seiko Epson Corp., Nagano, Japan) was used to print a mask on A4 paper to mark droplets that would be collected with toothpicks.

Silanization of petri dishes with APTES. Petri dishes for droplet storage were plasma cleaned with an oxygen plasma cleaner (model PDC-002; Harrick, Ithaca, NY) and filled with 15 ml of 2% APTES in ethanol and baked on a 50°C hot plate for 30 min. The surfaces were rinsed with ethanol and blow dried with nitrogen gas. The dishes were then baked in a 65°C oven for 30 min. The effect of silanization on surface flatness was evaluated with an atomic force microscope (Bruker, Billerica, MA).

Fabrication and operation of devices. PDMS-based microfluidic devices for droplet generation were made by soft lithography (30). Teflon tubing (200-μm inner diameter [i.d.], 250-μm outer diameter [o.d.]) was inserted into the junction of the microfabricated channels (see Fig. S3C in the supplemental material) and sealed with capillary wax (Hampton Research, Aliso Viejo, CA). Capillary-based devices were assembled with fused-silica capillaries (40-μm i.d., 100-μm o.d.) and Teflon tubing (200-μm i.d., 250-μm o.d.). Streaking tips coupled with droplet generation devices were made by fixing Teflon tubing within a pipette tip (200-μl size) with capillary wax. The end of the tubing was leveled with the conical tip to contact the surface of the dish during streaking. Syringe pumps controlled by the LabVIEW program were used to drive the fluid flow in devices. The streaking tip was operated manually or fixed on the automated dish drive (see Fig. 4A), lowered to contact a petri dish prefilled with mineral oil, and dragged across the surface of the petri dish along two-dimensional paths or spiral tracks; droplets exiting the Teflon tubing were left behind and formed a sessile-droplet array. The dish with a droplet array was covered with a lid and wrapped with Parafilm (Bemis, Neenah, WI). A wet filter paper ring was attached inside the lid to prevent long-term evaporation of droplets (see Fig. S1 in the supplemental material). The paper ring was soaked with deionized water. During incubation, the paper ring was replenished with water every other day. For additional details of the construction of the apparatus used and the operation of the MSP method, see Fig. S2 to S4 and the text in the supplemental material.

Preparation of bacterial samples. The bacterial species used were *Escherichia coli* RP437 carrying plasmid DsRedT.4 tagged with red fluorescent protein (RFP), *E. coli* RP1616 carrying plasmid pACGFP1 (Clontech Laboratories, Palo Alto, CA) tagged with green fluorescent protein (GFP), and GFP-tagged *Pseudomonas aeruginosa* PAO1. The original RP437 and RP1616 strains without exogenous plasmids were kindly provided by J. S. Parkinson of the University of Utah. PAO1 was provided by Luyan Ma of the Institute of Microbiology, Chinese Academy of Sciences. The GFP-tagged RP1616 and RFP-tagged RP437 bacteria were cultivated in LB broth containing 100 μg/ml ampicillin. PAO1 was cultivated in LB broth without antibiotics. The number of cells was adjusted by dilution.

The PAH-degrading microbial community was collected from soil at an abandon coke plant in a suburb of Beijing, China. The community was maintained on mineral salts medium (MSM) containing K_2HPO_4 at 1.60 g/liter, KH_2PO_4 at 0.40 g/liter, NH_4NO_3 at 1.0 g/liter, $MgSO_4{\cdot}7H_2O$ at 0.2 g/liter, $CaCl_2{\cdot}2H_2O$ at 0.10 g/liter, NaCl at 0.10 g/liter, and $FeCl_3{\cdot}6H_2O$ at 0.01 g/liter with 2 ml of a trace element solution containing MoO_3 at 4 g/liter, $ZnSO_4{\cdot}5H_2O$ at 28 g/liter, $CuSO_4{\cdot}5H_2O$ at 2 g/liter, H_3BO_3 at 4 g/liter, $MnSO_4{\cdot}5H_2O$ at 4 g/liter, and $CoCl_2{\cdot}6H_2O$ at 4 g/liter. This MSM was supplemented with fluoranthene for selection of PAH-degrading populations and was adjusted to an initial pH of 7.0 with HCl or NaOH. To make MSM-fluoranthene medium, 3 ml of a dichloromethane (DCM) stock solution of sterile fluoranthene (2,000 mg/liter) was added to autoclaved flasks. After the DCM had evaporated, 30 ml of MSM was transferred to the flasks to a final fluoranthene concentration of 200 mg/liter. All solid media were solidified with agar at 15 g/liter.

Isolation and cultivation of *E. coli*. Both *E. coli* strains were cultivated in LB broth containing 100 μg/ml ampicillin at 200 rpm/min at 37°C overnight, diluted 10,000 times with LB medium, and mixed 1:1 as the water phase in droplets streaking with an automated dish drive. The spiral droplet array was imaged with FITC and G-2A filters on the fluorescence microscope every 30 min for 24 h. To collect GFP-tagged RP1616 selectively from the droplet array, the droplet array was imaged and analyzed to find coordinate points in the *x*-*y* plane of all droplets as regions of interests. Those droplets with RP1616 (green) were selected according to GFP intensity and printed as black dots on paper. This paper was attached under the dish and aligned to make all droplets containing RP1616 coincide with the dots on the paper. Autoclaved toothpicks were used to transfer the RP1616 droplets and inoculate them onto an agar plate or into LB broth for scale-up growth. (see Fig. S6 in the supplemental material).

MIC determination. PAO1 was grown in LB broth at 200 rpm at 37°C. The cell suspension was first adjusted to an OD_{600} of 1 and then diluted 100 times with LB broth as the cell sample. Mineral oil was used as the carrier oil. Pure LB and LB with colistin at 100 μl/ml were used as the other two aqueous phases. For more precise control of the concentration, we added a 15-s prerun step with flow rates of the cell suspension, colistin, and LB broth set at 1.5, 0, and 1.5 μl/min, respectively. After the prerun step, we paused all of the pumps for 20 s while keeping the dish drive running and then initiated the ramping program. The flow rate of colistin was linearly ramped from 0 to 1.5 μl/min in 8 min, and the flow rate of LB broth was linearly decreased from 1.5 to 0 μl/min simultaneously, while the flow rate of PAO1 remained 1.5 μl/min and the carrier oil flow rate

was 20 μl/min. The device was fixed on the MSP system to generate a spiral array from an i.d. of 15 mm to an o.d. of 65 mm at a 5,000-μm/s constant linear velocity (CLV) (31) with a track spacing of 900 μm and a total writing time of 8 min. Control experiments (broth dilution method) were conducted with tubes containing colistin concentrations ranging from 0 to 80 μg/ml. Growth of PAO1 cells in tubes was observed for MIC evaluation.

Isolation and cultivation of bacteria from the PAH-degrading community. The PAH-degrading community was cultured with MSM-fluoranthene for approximately 3 days at 30°C to the postexponential growth phase (approximately 5×10^8 to 6×10^8 cells/ml) and diluted to a concentration of approximately 3×10^4 to 5×10^4 cells/ml as the sample. To isolate PAH-degrading species from the community, we performed experiments with MSP and agar plates simultaneously and three different culture media, i.e., LB broth, MSM containing 2 mmol/liter DHB, and MSM-fluoranthene. For the MSP method, instead of MSM-fluoranthene, we dissolved fluoranthene in mineral oil at a concentration of 200 mg/liter. By the MSP method, about 4,000 droplets from a cell suspension diluted in MSM were written onto the surfaces of petri dishes with ~30 μl of cell suspension. The same volume (30 μl) of inoculum was diluted with deionized water to 300 μl and spread onto agar plates in the same way as for the MSP method. All MSPs and agar plates were incubated at 30°C. Droplets containing growing cells, as well as visible colonies on agar plates, were harvested individually into 96-well plates, each well of which contained 200 μl of MSM-fluoranthene medium. After another 3 days of culture at 30°C monitored with Microbiology Reader Bioscreen C (Labsystems, Helsinki, Finland), the culture solutions were diluted to 10^{-4} to 10^{-6} according to their OD_{600}. Two-hundred-microliter diluents of each well were spread onto MSM-fluoranthene agar plates to obtain pure clones.

Identification of isolates from the PAH-degrading community. Single colonies on agar plates were picked and put into 0.2-ml tubes with 2 μl of lysate (Zomanbio, Beijing, China) and 150 μl of double-distilled H_2O (ddH_2O), and 2 μl was taken for PCR after stirring. PCR amplifications were carried out in a final 50-μl reaction volume that contained 2 μl of template DNA, 1 μl of each primer, 5 μl of 10× *Taq* buffer, 4 μl of a deoxynucleoside triphosphate mixture (200 mM each dATP, dCTP, dGTP, and dTTP), 0.5 μl of 25 U of *Taq* DNA polymerase, and 36.5 μl of ddH_2O. PCR amplification was conducted with the following program: predenaturation at 95°C for 10 min; 30 cycles of denaturation at 95°C for 1 min, annealing at 55°C for 1 min, and extension at 72°C for 1.0 min; and then 10 min of extension at 72°C. PCR products were purified on agarose gel, the bands were cut out, and DNA was extracted with the QIAquick gel extraction kit (Qiagen, Shanghai, China) and sequenced. Sequencing data were compared with 16S rRNA gene sequences available in the NCBI database (http://www.ncbi.nlm.nih.gov/) by BLAST searching.

Metagenomic sequencing. To evaluate the overall microbial diversity after cultivation, cells on agar plates or MSPs were pooled and total DNAs were extracted and PCR amplified with the U515F and 806R primers (16S rRNA gene V4 region) containing barcodes at the 5′ end of the forward primer. The PCR products were used to construct DNA libraries and sequenced on a MiSeq machine by the PE250 protocol. More than 30,000 raw sequences were obtained from each sample. See the supplemental material for details.

RESULTS

Concept, design, and work flow. Conventional petri dishes filled with agar media provide continuous space and nutrients for microbial cells to grow and develop into colonies. When an agar plate is inoculated with a complex microbial community, abundant and fast-growing microbes grow and consume nutrients and spread out rapidly, while rare or slow-growing microbes are adversely affected because of nutrient depletion and space limitation or even inhibited by metabolic exudates from the faster-growing microbes (19). Dilution plating allows the growth of some slow-growing

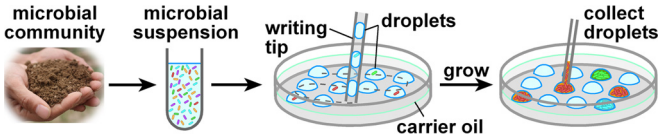

FIG 1 Work flow for microbial isolation from a mixture based on the MSP method.

microbes after long-term incubation. However, it requires a large number of plates to be screened to obtain isolates of rare species, which is labor-intensive and time-consuming. We predicted that if the space of a petri dish were separated into microspaces and nutrients were introduced into each microspace in a discontinuous way, the growth of microbial cells would be contained in the microspace, preventing fast-growing microbes from dominating the entire dish. On the basis of this idea, we developed the MSP method (Fig. 1). The MSP work flow features three major steps. In the first, a microfluidic device generates droplets of picoliter to nanoliter volumes carrying single microbial cells and transports them to the "writing tip." In the second, the droplets form stationary droplet arrays on the PS surface of an empty petri dish prefilled with carrier oil. In the third, the droplets are incubated during immersion in carrier oil to allow cells to grow and these cells can later be transferred for further cultivation or characterization.

Formation and stabilization of sessile-droplet arrays. The formation of a droplet array relies on spontaneous coalescence of the droplets with a surface. The coalescence time of droplets flowing toward a hydrophilic surface within carrier oil is reported to be a linear function of the capillary number (32), which defines the ratio of viscous energy over surface energy as $Ca = \mu_o U/\gamma$, where U (in meters per second) is the average flow velocity in the channel, μ_o (in pascal seconds) is the viscosity of the carrier oil (μ = 0.03 Pa · s for mineral oil), and γ (in newtons per meter) is the surface tension. Our results were consistent with this rule. For a writing tip with an i.d. of 200 μm and a flow velocity of 10 mm/s, droplets could spontaneously coalesce without the addition of a surfactant (e.g., Span 80) to the mineral oil (Ca = 0.006). After Span 80 (0.5%, wt/vol) was added to the mineral oil, Ca increased to 0.064 because of a decrease in surface tension (γ; from 50 to 4.67 mN · m^{-1}) (33). In this case, drifting of droplets away from the writing track was observed, which resulted in droplet coalescence and disruption of the array pattern. We also verified that the MSP system is compatible with silicone oil for droplet writing and storage.

PS petri dishes are ideal for storing a large quantity of droplets. They are affordable and widely available and provide a large surface area, high flatness, and optical transparency. To stabilize the droplet array and avoid optical distortion, we silanized the dish with APTES (Fig. 2A) (34). The average contact angles of 2 μl of LB broth before and after APTES modification were 161° (Fig. 2B) and 81°and (Fig. 2C). Our results showed that aqueous droplets drifted on the untreated PS surface and could not form a stable array (Fig. 2D). The spherical shape of droplets on the untreated surface also caused distortion during optical imaging (see Fig. S1D in the supplemental material). After silanization, we obtained moderate hydrophobicity for reliable and compact array storage of hemispherical nanoliter droplets (Fig. 2E), which allowed microbial cells inside droplets to be imaged and counted with high fidelity (see Fig. S1E in the supplemental material).

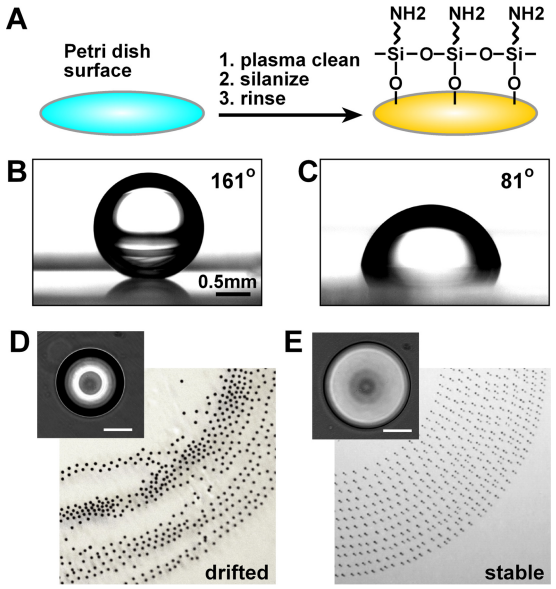

FIG 2 Stabilization of the droplet array. (A) Procedure used to introduce amine groups to PS petri dishes by silanization. (B to E) Photographs of 2-μl LB droplets deposited and micrographs of 7-nl droplets in the array written on the surface under mineral oil before (B, D) and after (C, E) silanization.

Under mineral oil, droplets evaporate very slowly and can be stored for several hours without a notable volume change. For long-term storage, the dish was covered with a lid attached with a polyester paper ring soaked with deionized water (see Fig. S1F and G in the supplemental material), and the paper ring was replenished with water every other day. This helped increase humidity, and the droplets could be stored for more than 1 month without drying up.

Manual streaking. To facilitate high-throughput cultivation of microbes in droplets, we made a capillary-based device. The device was composed of a droplet generator and a writing tip (Fig. 3). Monodisperse droplets with an average volume of 6.2 nl (relative standard deviation [RSD] = 0.97%; $n = 10$) were obtained in the Teflon tubing when the flow rates of the sample (food dye) and the oil in the droplet generator were 3 and 30 μl/min, respectively (Fig. 3C). The writing tip was manually moved in a zigzag pattern over a dish prefilled with ~15 ml of mineral oil (~3 mm thick). Droplets instantly coalesced on the surface of the dish along the moving track. A typical manually written droplet array was generated in 4 min by manual streaking (Fig. 3D). The final array contained more than 1,800 food dye droplets.

Automated streaking. Inspired by the compact disc digital data storage scheme (31), we designed a low-cost and automated dish drive to further improve the efficiency and capacity of storage. The dish drive contains a spindle motor carrying the dish and a linear translator holding the microfluidic device (Fig. 4A and B). The spindle motor spins the dish, the linear translator moves along a radius away from the center of the dish, and the droplets exiting the writing tip are written on spiral tracks with a uniform spatial distribution on the dish, forming a large-scale array of sessile droplets that can be monitored, indexed, and individually accessed. The spiral tracks of droplets were deposited with a CLV, obtaining uniform and compact droplet distribution. We could easily address the droplet array by imaging and indexing droplets with their positions in the spiral tracks. For additional details of the CLV model and the construction of the dish drive, see Fig. S2 in the supplemental material.

Addressable spiral array for high-throughput experiments. We investigated whether variable constituents could be encoded in the addressable droplet array. We used T-junction geometry (30, 35) to generate droplets with an arbitrary mixing ratio and wrote the droplet array by automated streaking. Using three food dye solutions (red, yellow, and blue) for the demonstration, we performed three-component dosing and mixing (Fig. 4; see Fig. S3 in the supplemental material). The resultant droplet array contained more than 1,600 droplets with colors continuously changing (Fig. 4D).

We used the MSP method to measure the inhibition effect of the antibiotic colistin sulfate against GFP-tagged PAO1, a Gram-negative opportunistic human pathogen with multidrug resistance. Colistin is one of the last-resort antimicrobial drugs for bacterial infections. Determination of the MIC of colistin is important for improving outcomes for patients and preventing the evolution of drug-resistant strains. A total of 2,261 droplets of 6 nl containing PAO1 cells, culture medium, and colistin in LB broth were generated and written onto a petri dish. The final droplets contained about 50 PAO1 cells each, and colistin concentrations ranged from 0 to 100 μg/ml, controlled by linear ramping up of the flow rate of colistin opposite to that of the culture medium. The droplet array was imaged with a motorized microscope every hour (Fig. 4F). The fluorescence intensities of droplets at 24 h were plotted against the concentrations of colistin and exhibited a monophasic dose-response curve (Fig. 4G). The MIC for 99% of the bacterial cells tested (MIC_{99}) was 72.7 μg/ml. This result is in agreement with control experiments with well plates, which produced a MIC_{99} of 70 μg/ml.

To achieve a greater storage capacity, we fabricated a PDMS device that generates droplets with a 180-pl volume based on flow focusing design, with the droplet exit channel (60 by 60 μm in size) carefully trimmed to serve as the writing tip (see Fig. S4 in the supplemental material). The device was fixed on the automated

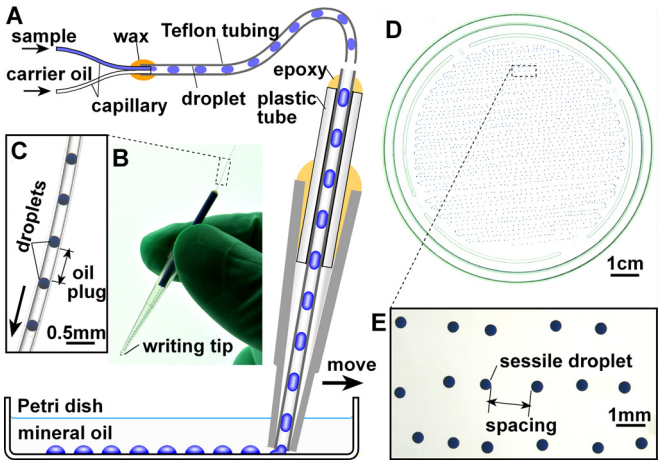

FIG 3 Manual droplet streaking. (A) Schematic of a capillary-based device for writing droplets on a petri dish prefilled with mineral oil. (B) Photograph of the manual writing tip. (C) Close-up view of droplets flowing in Teflon tubing toward the writing tip. (D) Sessile-droplet array produced by manual streaking onto a petri dish. (E) Close-up view of the sessile-droplet array showing uniform footprint sizes.

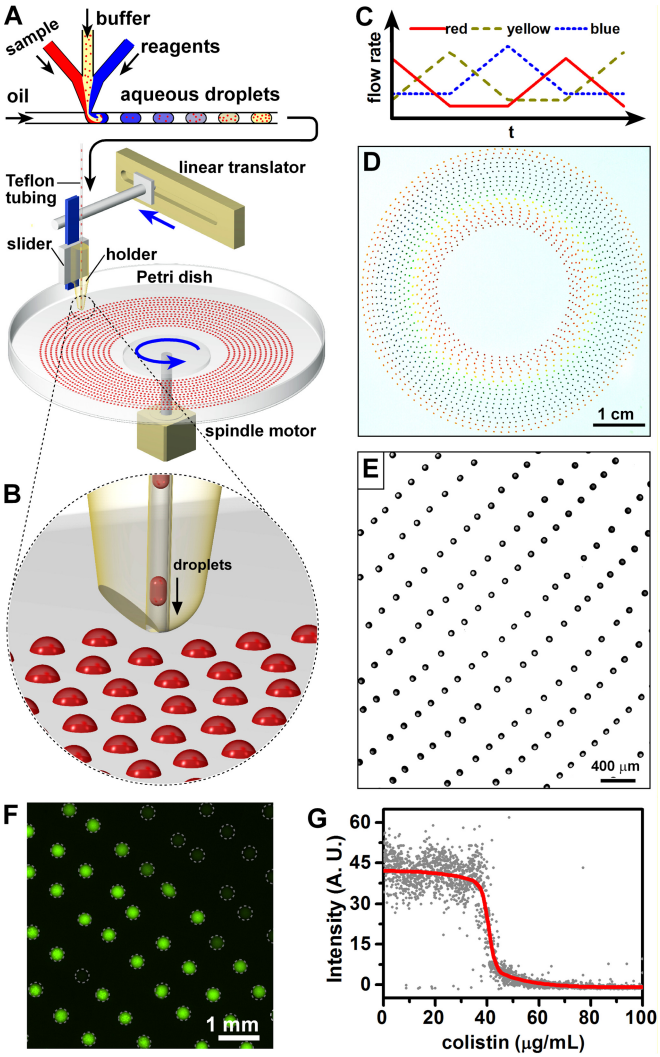

FIG 4 Automated droplet streaking and application to antimicrobial susceptibility testing. (A) Schematic of a microfluidic device and automated dish drive for generating spiral droplet arrays. (B) Close-up view of continuous droplet deposition by a writing tip. (C) The program for serial dilution and mixing of red, yellow, and blue food dyes in droplets generated in sequence. (D) The resulting spiral droplet array with rainbow colors. (E) Micrograph showing a typical region of a spiral array of 180-pl droplets. (F) Testing of *P. aeruginosa* PAO1 susceptibility to colistin at concentrations increasing from 0 (inner tracks) to 100 (outer tracks) μg/ml. The green fluorescence micrograph of a typical region of the droplet array is shown, and droplets are outlined with white dots. (G) Integrated fluorescence intensity of 2,261 droplets with colistin concentrations ranging from 0 to 100 μg/ml. A.U., arbitrary units.

dish drive to generate droplets and write droplets from an i.d. of 10 mm to an o.d. of 75 mm at a CLV of 5,000 μm/s and a track spacing of 400 μm. About 50,000 180-pl droplets were written on the dish in 36 min (Fig. 4E). The storage capacity is scalable, as we can use larger petri dishes to expand the storage area.

Single-cell isolation and cultivation of *E. coli*. To demonstrate the capacity of MSP for single-cell separation and cultivation, we prepared a sample consisting of GFP-tagged RP1616 and RFP-tagged RP437. Both strains were cultivated overnight, diluted 10,000 times in LB broth, and mixed 1:1 for use as the "ink" to write a droplet array by automated streaking. An array of 4,115 droplets (~6 nl) on a petri dish was obtained (Fig. 5A and B). The representative growth pattern of single RP1616 cells in a droplet is shown in Fig. 5C. Typical single-cell growth curves of RP1616 and RP437 were monitored by imaging at 30-min intervals for 22 h (see Fig. S5 in the supplemental material). After 24 h of incubation at 37°C, about 38.0% of the droplets contained growth of only RP1616 (green) or only RP437 (red) and 3.5% contained growth of both strains (Fig. 5B).

Targeted recovery of bacterial species from MSPs. We optimized the sessile droplets to ~300 μm (6 to 7 nl) with 700- to 1,000-μm spacing for easy observation and operation. To select droplets for further cultivation, the droplet array was imaged and then all droplets with GFP-tagged RP1616 were marked with a mask (printed on paper with an inkjet printer) aligned under the petri dish with the help of a stereoscope (Fig. 6). We carefully picked 144 droplets that contained GFP-tagged *E. coli* with sterile toothpicks. Cells from 131 droplets were successfully transferred to and grown on fresh agar plates, showing that 91% of the cells in droplets were successfully harvested and scaled up (Fig. 6).

Isolation and cultivation of fluoranthene-degrading species. PAH have raised serious environmental and health concerns because of their toxicity to animals and humans and their persistence in the environment. Microbial degradation is a major process used to remediate PAH-polluted sites (36). However, isolation and cultivation of PAH-degrading species on conventional agar plates are labor-exhaustive and often unsuccessful, partly because of the hydrophobic nature of PAH (very low solubility in water). Recently, we enriched a microbial community from a PAH-polluted site (37) that could effectively degrade 95.12% of the fluoranthene in MSM after 9 days (see Fig. S6 in the supplemental material). Results of 16S rRNA gene metagenomic sequencing revealed that the community was composed of >190 operational taxonomic units (OTUs) with a high degree of variation in abundance.

To recover PAH-degrading species from this soil community, we used the conventional method and the MSP method in parallel (Fig. 7A). A 30-μl inoculum of the community in MSM broth (30 μl) was written as ~4,000 droplets on petri dishes prefilled with mineral oil. The inoculating cell density was controlled to yield ~20 to 30% of droplets carrying microbial cells. Fluoranthene was dissolved in mineral oil at 200 μg/ml to serve as the carbon source. By this approach, fluoranthene was continuously supplied by diffusion for cell growth in the droplets, thus avoiding the toxicity of higher concentrations of fluoranthene (Fig. 7B). Microbial growth in droplets was monitored by time-serial imaging, showing that the community contained both fast- and slow-growing species (Fig. 7C). The droplets were incubated, and those in which microbes grew were harvested and transferred into MSM supplemented with fluoranthene as the sole carbon source. At the same time, a 30-μl inoculum of the community was diluted with deionized water to 300 μl and spread on MSM-fluoranthene agar plates for cultivation and isolation. The degradation of fluoranthene by each isolate was evaluated by determination of fluoranthene removal (see Table S1 in the supplemental material).

In the original community, the average *Mycobacterium* 16S rRNA gene abundance reached 20.4% (see Table S2 in the supplemental material), which indicated that *Mycobacterium* might be one of the dominant PAH-degrading genera. However, the fluoranthene degradation rates all of the isolates obtained from agar plates were in a low range of <12.7% after 9 days (Fig. 7) and no

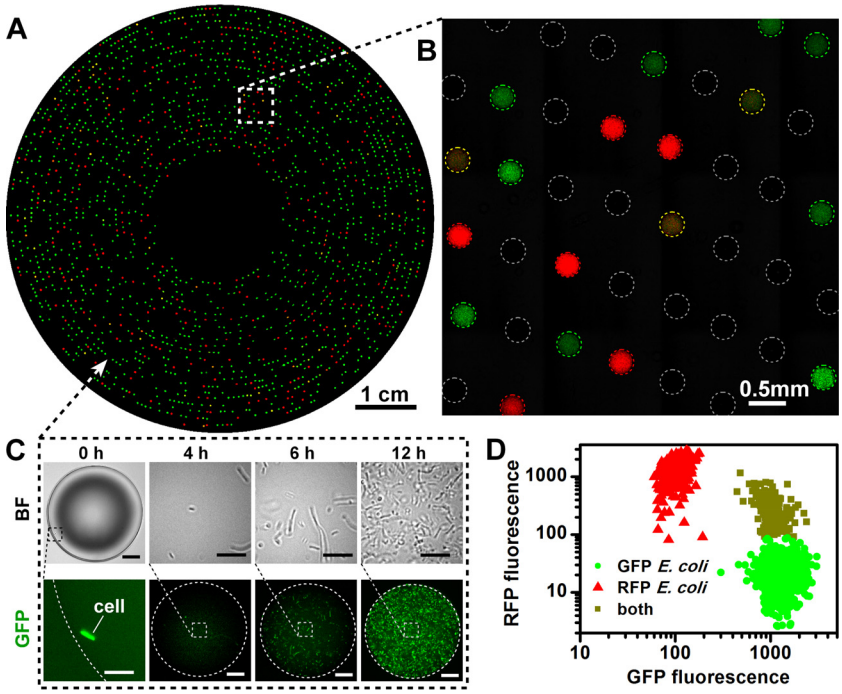

FIG 5 Isolation and cultivation of bacterial cells from a mixture of RFP-tagged *E. coli* RP437 and GFP-tagged *E. coli* RP1616. (A, B) Overlaid green and red fluorescence images of the droplet array after 24 h of cultivation. Droplets are outlined with white dots. (C) Time-lapse micrographs of green fluorescence showing the growth of single RP1616 cells in a droplet. The scale bars are 50 μm for droplets and 5 μm for close-up views. Dots outline the edges of droplets. BF, bright field. (D) Scatter plot of green and red fluorescence of droplets with growth of only RP1616, only RP437, or a mixture of both strains.

Mycobacterium isolates were found. With fluoranthene as the sole carbon source, microscopic imaging revealed that *Mycobacterium* strains isolated from MSP were slow-growing bacteria with long doubling times (Fig. 7C). Their low growth rates might result in small colony sizes on agar when they are mixed with fast-growing species. As expected, by the MSP method, we obtained four *Mycobacterium* isolates that could effectively remediate fluoranthene at 94.6 to 99.5% degradation rates in 9 days (Fig. 7D; see Fig. S6 in the supplemental material). Moreover, we obtained an isolate of the genus *Blastococcus* with DHB as the carbon source that could degrade 100% of the fluoranthene present after 9 days (Fig. 7D). Unexpectedly, the genus *Blastococcus* was not detected by 16S rRNA gene sequencing of the original community, indicating that it belongs to the rare biosphere. These results indicate that the MSP method effectively eliminates interspecies competition and provides a significant advantage in isolating microbial species that are commonly overlooked by conventional methods.

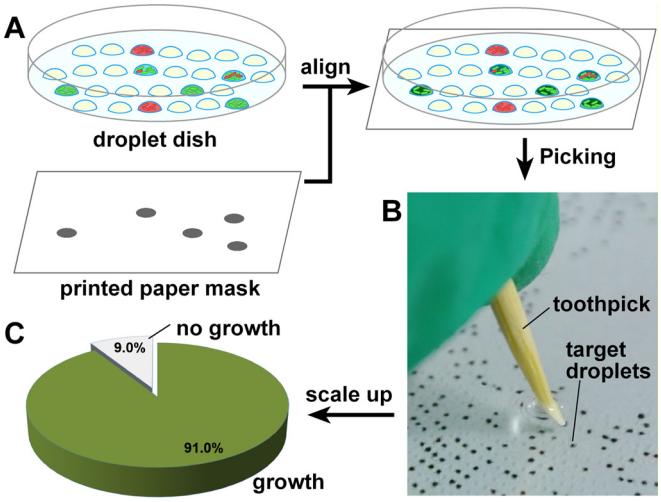

FIG 6 Rapid recovery of microbial cells from MSPs after growth. (A) The coordinate positions of droplets that contain *E. coli* RP1616 cells were printed on paper as black dots. This paper was attached under the dish, and droplets were aligned with the dots for selective picking. (B) Picking of a droplet coordinate with a black dot with a toothpick for scale-up cultivation. (C) The success rate of droplet picking evaluated by growth of RP1616. A total of 144 droplets were picked, and 131 droplets were successfully scaled up with growth of RP1616 on an agar plate.

Approaching the microbial diversity of the PAH-degrading community. Unraveling the vast diversity of complex microbial communities is challenging for both culture-dependent and culture-independent methods. In addition to isolating and characterizing individual species, we also demonstrated that the total biomass on each MSP dish can be easily pooled and subjected to 16S rRNA gene sequencing to elucidate overall "cultivable" microbial diversity. To compare the MSP and agar plate methods, parallel cultivation of the same soil community was carried out; for the results, see Table S2 in the supplemental material. All experiments were performed in triplicate. Principal-coordinate analysis revealed that cultivation is robust and reproducible (see Fig. S7 in the supplemental material). Sequencing indicated that both the MSP and agar plate methods were successful in the recovery of major taxa. However, the MSP method led to higher microbial diversity than the agar plate method. Rarefaction curves suggested that OTU richness from MSPs was about 22.2% greater than that from agar plates (Fig. 7E). Relative 16S rRNA gene abun-

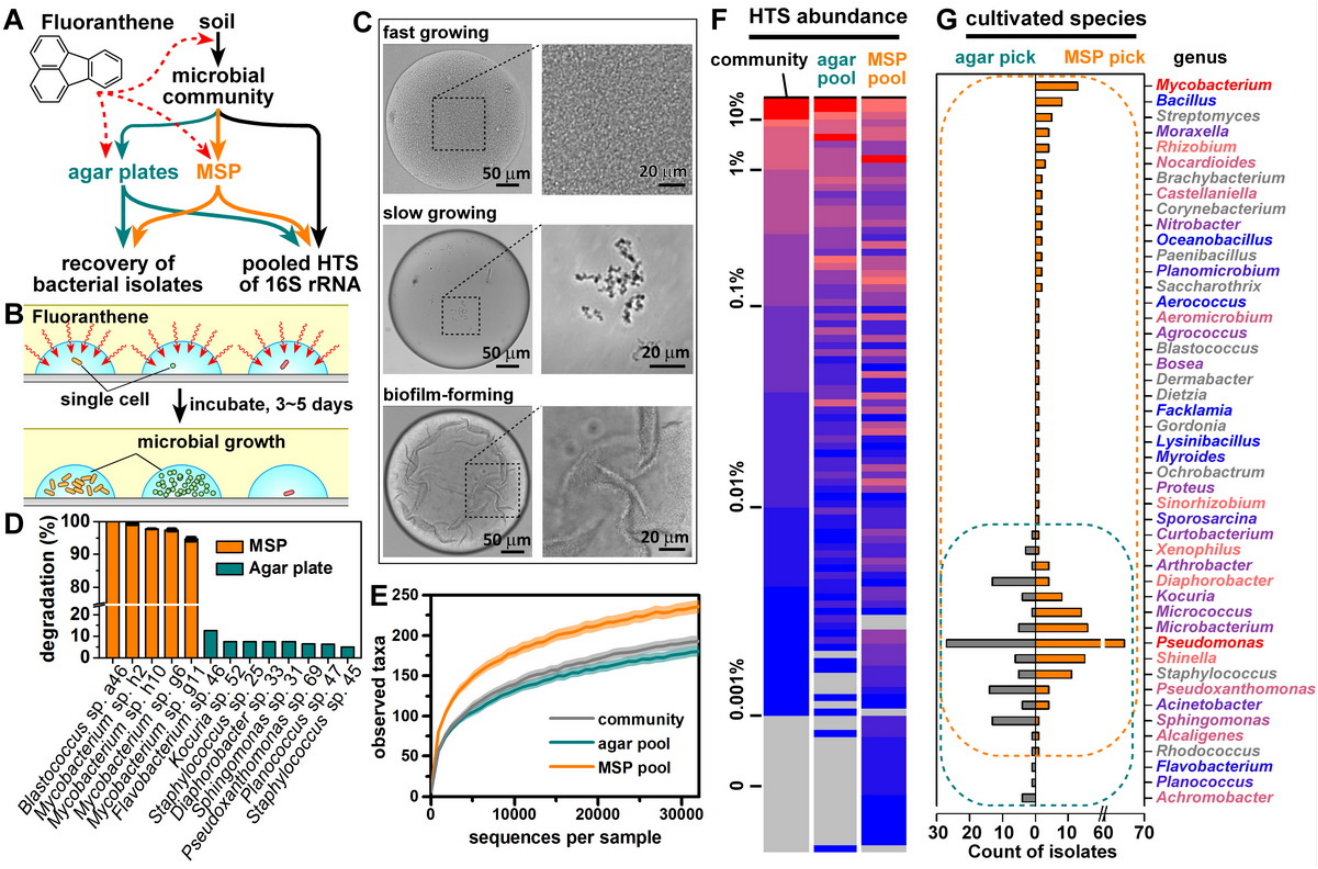

FIG 7 Isolation and characterization of a PAH-degrading community enriched from petroleum-contaminated soil. (A) Diagram of metagenomic DNA library construction and strain isolation with agar plates and MSPs. (B) Schematic of single-cell isolation and cultivation in droplets with MSM with fluoranthene supplied from mineral oil as the carbon source. (C) Typical micrographs of fast-growing, slow-growing, and biofilm-forming species. (D) Ranking of fluoranthene-degrading efficiencies of pure strains obtained by MSPs and agar plates according to fluoranthene removal in 9 days. (E, F) Rarefaction curves (E) and heat maps (F) of metagenomic sequencing of the original community, pooled cells from agar plates, and pooled cells from MSPs. Fluoranthene was used as the sole carbon source. (G) Cultivated isolates from MSPs and agar plates with genus names colored according to the metagenomic abundance of the community in various culture media. HTS, high-throughput sequencing.

dance shows that MSP significantly increased the chance of rare species detection by sequencing (Fig. 7F), maybe because MSP allowed some rare species to grow from single cells with sufficient nutrients and space and without suppression by fast-growing species.

We explored microbial cultivation by conventional agar plate and MSP methods in parallel. In total, we obtained and characterized 105 isolates on agar plates and 218 isolates by the MSP method and performed 16S rRNA gene sequencing of individual isolates. A total of 47 OTUs (at the genus level) were recovered from the PAH-degrading community (Fig. 7G). The agar plate method recovered 18 of these, and the MSP method recovered 44. The coverage of species diversity for agar plates and MSP droplets was estimated to be 89.2 and 68.1%, suggesting that the diversity recovered from agar plates and droplets could be further improved and that the MSP method has the potential to detect even greater richness if more isolates are sampled. A total of 55 microbial isolates of 24 OTUs obtained by the MSP method had a relative abundance of <0.1% (in the original community), which demonstrated again that the MSP method has an advantage in cultivating members of the rare biosphere.

DISCUSSION

We developed a simple microfluidic method for the continuous generation of large-scale droplet arrays. The novelty of this method lies in the robustness of surface modification, the simple chip-to-world interface design, its high speed and high throughput capacity, and the simple streaking and picking strategies. Previous methods of generating droplet arrays usually involved precise position configuration, either predefined by robots or with the help of microfabricated chambers (38–40). These methods result in remarkably accurate positioning and provide additional capabilities, including automated multistep liquid handling. However, the widespread applicability of these systems has been limited by the complexity required to attain precise alignments, stop-flow modulation, and a microfabricated array structure (38, 39). We took advantage of the fact that in microchannels, adjacent droplets are spaced by uniform oil plugs during formation and flow. As the writing tip is moved across the surface of the petri dish, adjacent droplets coalesce with the surface and are separated by a distance that can be tuned by the time interval and velocity of the writing tip. Although the spiral array structures obtained in this work are not as uniform and conve-

nient as those of a standard rectangular array in terms of manipulation and detection, our method is much simpler than existing robotic systems and can effectively use the surfaces of petri dishes, which are commonly round.

The MSP method effectively reduces the labor, time, and cost required to perform high-throughput cultivation of cells and can be set up easily in common laboratories. Working from the conventional plate-streaking technique, the MSP method could be applied to microbial cultivation in a way similar to traditional microbial cultivation on agar plates. Droplet storage on a disposable petri dish prefilled with carrier oil provides long-term stabilization and biocompatibility. Cells grown in droplets can be easily harvested with toothpicks and transferred. Full automation of the MSP method may be realized with commercially available motorized colony pickers, though these systems are currently very expensive. We believe that the MSP work flow could be used with various droplet-based microfluidic systems to facilitate many applications, such as studies of cellular heterogeneity (41), selection of mutants, and adherent-cell or microbial biofilm cultivation. In addition, the spiral droplet array generated by an automated dish drive is addressable, which facilitates serial dilution and dose-response screening. In this work, the fluoranthene dissolved in the hydrophobic carrier oil diffused continuously into the aqueous droplets, thus supporting microbial cell growth and promoting the recovery of microbial species with high degradation efficiency. This method could be further extended by appropriate combinations of the carrier oil phase, such as by using lipids, petroleum, and hydrophobic substrates that dissolve in the oil phase, such as water-insoluble herbicides, pesticides, or other hydrophobic environmental pollutants, enabling the isolation and identification of functional microbes for bioremediation and bioconversion.

"Who are out there, and what are they doing?" These are the most fundamental and persistent questions for environmental microbiology. Major challenges in gaining this knowledge include the following. (i) Many microbes are recalcitrant to cultivation, and our knowledge of their physiology is limited. (ii) Slow-growing and rare microbes are often masked by more abundant species during cultivation and sequencing. (iii) Some microbes cannot be grown alone because their growth depends on another microbe's metabolic activity or on environmental conditions. By the simple MSP approach, the cultivation area of a petri dish is divided into large numbers of droplets to allow the segregation of species in very low numbers and provide space and nutrients for single microbial cells to grow, while separation among droplets prevents fast-growing strains and more abundant species from outcompeting slow-growing strains and rare species. Droplets can be pooled for metagenomic analysis to allow the rapid evaluation of various substrates and culture conditions for the recovery of species with different metabolic lifestyles. In this study, we have demonstrated that application of the MSP significantly increases the diversity of the microbes recovered. We found that MSP greatly improved the efficiency of isolation and cultivation of rare species, including the discovery of a previously unknown fluoranthene-degrading *Blastococcus* species that was not detected by sequencing. This finding proves that the rare biosphere may contain a multitude of undiscovered biochemical capabilities that are highly relevant in biotechnological applications (4). In this work, we evaluated several hundred isolates from a soil community. New methods for rapid and cost-effective characterization of microbial isolates have to be introduced for comprehensive studies of complex microbial communities. Another interesting direction for future work is the dilution of communities to multiple cells per droplet (42) or to single cells accompanied by externally added syntrophic species in droplets for isolation of novel strains with symbiotic interactions (43). We envision that the MSP work flow described in this paper can be useful for harnessing microbial diversity and recovering functional and rare biosphere members relevant to host health, biogenic transformation, and natural products.

ACKNOWLEDGMENTS

We thank Natasha Shelby and Liang Ma for help in editing the manuscript.

We declare no conflict of interest.

FUNDING INFORMATION

This work is supported by the National Natural Science Foundation of China (31230003, 21205134, 21377161, and 31470221), the program of China Ocean Mineral Resources R&D Association (DY125-15-R-02), the Strategic Priority Research Program of Chinese Academy of Sciences (XDB15040102), and the National High Technology Research and Development Program of China (2012AA092103).

REFERENCES

1. **Daniel R.** 2005. The metagenomics of soil. Nat Rev Microbiol **3:**470–478. http://dx.doi.org/10.1038/nrmicro1160.
2. **Li J, Jia H, Cai X, Zhong H, Feng Q, Sunagawa S, Arumugam M, Kultima JR, Prifti E, Nielsen T, Juncker AS, Manichanh C, Chen B, Zhang W, Levenez F, Wang J, Xu X, Xiao L, Liang S, Zhang D, Zhang Z, Chen W, Zhao H, Al-Aama JY, Edris S, Yang H, Wang J, Hansen T, Nielsen HB, Brunak S, Kristiansen K, Guarner F, Pedersen O, Dore J, Ehrlich SD, Bork P, Wang J.** 2014. An integrated catalog of reference genes in the human gut microbiome. Nat Biotechnol **32:**834–841. http://dx.doi.org/10.1038/nbt.2942.
3. **Whiteley AS, Bailey MJ.** 2000. Bacterial community structure and physiological state within an industrial phenol bioremediation system. Appl Environ Microbiol **66:**2400–2407. http://dx.doi.org/10.1128/AEM.66.6.2400-2407.2000.
4. **Fuhrman JA.** 2009. Microbial community structure and its functional implications. Nature **459:**193–199. http://dx.doi.org/10.1038/nature08058.
5. **Galand PE, Casamayor EO, Kirchman DL, Lovejoy C.** 2009. Ecology of the rare microbial biosphere of the Arctic Ocean. Proc Natl Acad Sci U S A **106:**22427–22432. http://dx.doi.org/10.1073/pnas.0908284106.
6. **Huber JA, Mark WD, Morrison HG, Huse SM, Neal PR, Butterfield DA, Sogin ML.** 2007. Microbial population structures in the deep marine biosphere. Science **318:**97–100. http://dx.doi.org/10.1126/science.1146689.
7. **Stevenson BS, Eichorst SA, Wertz JT, Schmidt TM, Breznak JA.** 2004. New strategies for cultivation and detection of previously uncultured microbes. Appl Environ Microbiol **70:**4748–4755. http://dx.doi.org/10.1128/AEM.70.8.4748-4755.2004.
8. **Stewart, E. J.** 2012. Growing unculturable bacteria. J Bacteriol **194:**4151–4160. http://dx.doi.org/10.1128/JB.00345-12.
9. **Epstein SS.** 2013. The phenomenon of microbial uncultivability. Curr Opin Microbiol **16:**636–642. http://dx.doi.org/10.1016/j.mib.2013.08.003.
10. **Lagier JC, Armougom F, Million M, Hugon P, Pagnier I, Robert C, Bittar F, Fournous G, Gimenez G, Maraninchi M, Trape JF, Koonin EV, La Scola B, Raoult D.** 2012. Microbial culturomics: paradigm shift in the human gut microbiome study. Clin Microbiol Infect **18:**1185–1193. http://dx.doi.org/10.1111/1469-0691.12023.
11. **Brooks JP, Edwards DJ, Harwich MJ, Rivera MC, Fettweis JM, Serrano MG, Reris RA, Sheth NU, Huang B, Girerd P, Strauss JR, Jefferson KK, Buck GA.** 2015. The truth about metagenomics: quantifying and counteracting bias in 16S rRNA studies. BMC Microbiol **15:**66. http://dx.doi.org/10.1186/s12866-015-0351-6.
12. **Cardenas E, Tiedje JM.** 2008. New tools for discovering and characterizing microbial diversity. Curr Opin Biotechnol **19:**544–549. http://dx.doi.org/10.1016/j.copbio.2008.10.010.

13. **Lok C.** 2015. Mining the microbial dark matter. Nature **522:**270–273. http://dx.doi.org/10.1038/522270a.
14. **Morey M, Fernandez-Marmiesse A, Castineiras D, Fraga JM, Couce ML, Cocho JA.** 2013. A glimpse into past, present, and future DNA sequencing. Mol Genet Metab **110:**3–24. http://dx.doi.org/10.1016/j.ymgme.2013.04.024.
15. **Blainey PC, Quake SR.** 2014. Dissecting genomic diversity, one cell at a time. Nat Methods **11:**19–21. http://dx.doi.org/10.1038/nmeth.2783.
16. **Cho JC, Giovannoni SJ.** 2004. Cultivation and growth characteristics of a diverse group of oligotrophic marine *Gammaproteobacteria*. Appl Environ Microbiol **70:**432–440. http://dx.doi.org/10.1128/AEM.70.1.432-440.2004.
17. **Zengler K, Toledo G, Rappe M, Elkins J, Mathur EJ, Short JM, Keller M.** 2002. Cultivating the uncultured. Proc Natl Acad Sci U S A **99:**15681–15686. http://dx.doi.org/10.1073/pnas.252630999.
18. **Kaeberlein T, Lewis K, Epstein SS.** 2002. Isolating "uncultivable" microorganisms in pure culture in a simulated natural environment. Science **296:**1127–1129. http://dx.doi.org/10.1126/science.1070633.
19. **Ingham CJ, Sprenkels A, Bomer J, Molenaar D, van den Berg A, van Hylckama Vlieg JET, de Vos WM.** 2007. The micro-petri dish, a million-well growth chip for the culture and high-throughput screening of microorganisms. Proc Natl Acad Sci U S A **104:**18217–18222. http://dx.doi.org/10.1073/pnas.0701693104.
20. **Nichols D, Cahoon N, Trakhtenberg EM, Pham L, Mehta A, Belanger A, Kanigan T, Lewis K, Epstein SS.** 2010. Use of ichip for high-throughput *in situ* cultivation of "uncultivable" microbial species. Appl Environ Microbiol **76:**2445–2450. http://dx.doi.org/10.1128/AEM.01754-09.
21. **Ling LL, Schneider T, Peoples AJ, Spoering AL, Engels I, Conlon BP, Mueller A, Schaberle TF, Hughes DE, Epstein S, Jones M, Lazarides L, Steadman VA, Cohen DR, Felix CR, Fetterman KA, Millett WP, Nitti AG, Zullo AM, Chen C, Lewis K.** 2015. A new antibiotic kills pathogens without detectable resistance. Nature **517:**455–459. http://dx.doi.org/10.1038/nature14098.
22. **Lederberg J.** 1954. A simple method for isolating individual microbes. J Bacteriol **68:**258–259.
23. **Joensson HN, Andersson SH.** 2012. Droplet microfluidics—a tool for single-cell analysis. Angew Chem Int Ed Engl **51:**12176–12192. http://dx.doi.org/10.1002/anie.201200460.
24. **Martin K, Henkel T, Baier V, Grodrian A, Schon T, Roth M, Michael KJ, Metze J.** 2003. Generation of larger numbers of separated microbial populations by cultivation in segmented-flow microdevices. Lab Chip **3:**202–207. http://dx.doi.org/10.1039/b301258c.
25. **Liu W, Kim HJ, Lucchetta EM, Du W, Ismagilov RF.** 2009. Isolation, incubation, and parallel functional testing and identification by FISH of rare microbial single-copy cells from multi-species mixtures using the combination of chemistrode and stochastic confinement. Lab Chip **9:**2153–2162. http://dx.doi.org/10.1039/b904958d.
26. **Ma L, Kim J, Hatzenpichler R, Karymov MA, Hubert N, Hanan IM, Chang EB, Ismagilov RF.** 2014. Gene-targeted microfluidic cultivation validated by isolation of a gut bacterium listed in Human Microbiome Project's Most Wanted taxa. Proc Natl Acad Sci U S A **111:**9768–9773. http://dx.doi.org/10.1073/pnas.1404753111.
27. **Leung K, Zahn H, Leaver T, Konwar KM, Hanson NW, Page AP, Lo CC, Chain PS, Hallam SJ, Hansen CL.** 2012. A programmable droplet-based microfluidic device applied to multiparameter analysis of single microbes and microbial communities. Proc Natl Acad Sci U S A **109:**7665–7670. http://dx.doi.org/10.1073/pnas.1106752109.
28. **Shemesh J, Ben AT, Avesar J, Kang JH, Fine A, Super M, Meller A, Ingber DE, Levenberg S.** 2014. Stationary nanoliter droplet array with a substrate of choice for single adherent/nonadherent cell incubation and analysis. Proc Natl Acad Sci U S A **111:**11293–11298. http://dx.doi.org/10.1073/pnas.1404472111.
29. **Ma L, Datta SS, Karymov MA, Pan Q, Begolo S, Ismagilov RF.** 2014. Individually addressable arrays of replica microbial cultures enabled by splitting SlipChips. Integr Biol (Camb) **6:**796–805. http://dx.doi.org/10.1039/c4ib00109e.
30. **Li L, Mustafi D, Fu Q, Tereshko V, Chen DL, Tice JD, Ismagilov RF.** 2006. Nanoliter microfluidic hybrid method for simultaneous screening and optimization validated with crystallization of membrane proteins. Proc Natl Acad Sci U S A **103:**19243–19248. http://dx.doi.org/10.1073/pnas.0607502103.
31. **Lane PM, Van Dommelen R, Cada M.** 2001. Compact disc players in the laboratory: experiments in optical storage, error correction, and optical fiber communication. IEEE Trans Educ **44:**47–60. http://dx.doi.org/10.1109/13.912710.
32. **Liu Y, Ismagilov RF.** 2009. Dynamics of coalescence of plugs with a hydrophilic wetting layer induced by flow in a microfluidic chemistrode. Langmuir **25:**2854–2859. http://dx.doi.org/10.1021/la803518b.
33. **Sun M, Bithi SS, Vanapalli SA.** 2011. Microfluidic static droplet arrays with tuneable gradients in material composition. Lab Chip **11:**3949–3952. http://dx.doi.org/10.1039/c1lc20709a.
34. **Liu X, Yi Q, Han Y, Liang Z, Shen C, Zhou Z, Sun J L, Li Y, Du W, Cao R.** 2015. A robust microfluidic device for the synthesis and crystal growth of organometallic polymers with highly organized structures. Angew Chem Int Ed Engl **54:**1846–1850. http://dx.doi.org/10.1002/anie.201411008.
35. **Song H, Chen DL, Ismagilov RF.** 2006. Reactions in droplets in microfluidic channels. Angew Chem Int Ed Engl **45:**7336–7356. http://dx.doi.org/10.1002/anie.200601554.
36. **Kappell AD, Wei Y, Newton RJ, Van Nostrand JD, Zhou J, McLellan SL, Hristova KR.** 2014. The polycyclic aromatic hydrocarbon degradation potential of Gulf of Mexico native coastal microbial communities after the Deepwater Horizon oil spill. Front Microbiol **5:**205. http://dx.doi.org/10.3389/fmicb.2014.00205.
37. **Zhao J-K, Li X-M, Zhang M-J, Jin J, Jiang C-Y, Liu S-J.** 2013. *Parapedobacter pyrenivorans* sp. nov., isolated from a pyrene-degrading microbial enrichment, and emended description of the genus *Parapedobacter*. Int J Syst Evol Microbiol **63:**3994–3999. http://dx.doi.org/10.1099/ijs.0.051938-0.
38. **Du W, Sun M, Gu S, Zhu Y, Fang Q.** 2010. Automated microfluidic screening assay platform based on DropLab. Anal Chem **82:**9941–9947. http://dx.doi.org/10.1021/ac1020479.
39. **Zhou Y, Pang Y, Huang Y.** 2012. Openly accessible microfluidic liquid handlers for automated high-throughput nanoliter cell culture. Anal Chem **84:**2576–2584. http://dx.doi.org/10.1021/ac203469v.
40. **Küster SK, Fagerer SR, Verboket PE, Eyer K, Jefimovs K, Zenobi R, Dittrich PS.** 2013. Interfacing droplet microfluidics with matrix-assisted laser desorption/ionization mass spectrometry: label-free content analysis of single droplets. Anal Chem **85:**1285–1289. http://dx.doi.org/10.1021/ac3033189.
41. **Wang X, Kang Y, Luo C, Zhao T, Liu L, Jiang X, Fu R, An S, Chen J, Jiang N, Ren L, Wang Q, Baillie JK, Gao Z, Yu J.** 2014. Heteroresistance at the single-cell level: adapting to antibiotic stress through a population-based strategy and growth-controlled interphenotypic coordination. mBio **5:**e00942-13. http://dx.doi.org/10.1128/mBio.00942-13.
42. **Park J, Kerner A, Burns MA, Lin XN.** 2011. Microdroplet-enabled highly parallel co-cultivation of microbial communities. PLoS One **6:**e17019. http://dx.doi.org/10.1371/journal.pone.0017019.
43. **Cheng L, Ding C, Li Q, He Q, Dai LR, Zhang H.** 2013. DNA-SIP reveals that Syntrophaceae play an important role in methanogenic hexadecane degradation. PLoS One **8:**e66784. http://dx.doi.org/10.1371/journal.pone.0066784.

SUPPLEMENTAL TEXT.

Measurement of contact angle after aminosilanization. To measure the contact angle of polystyrene (PS) Petri dishes before and after silanization under mineral oil, Petri dishes were cut into 1 cm × 1 cm pieces, cleaned with ethanol and dried with nitrogen gas, and then immersed into mineral oil in a glass tank. 2 μL measured aqueous solution was carefully deposited on the surface. The contact angle of the droplet on the substrate was subsequently measured by using SL200B optical goniometer (SL200B, Shanghai, China). The same measurements were performed at least five times and the average contact angles were calculated.

Distortion-free imaging of sessile droplets. GFP-tagged *Pseudomonas aeruginosa* PAO1 was used to demonstrate the performance of sessile droplets on high resolution and distortion-free imaging. PAO1 was cultured in LB medium under 200 rpm/min at 37 ºC, adjusted to OD_{600}=1, and was diluted 200 times by LB medium as the cell suspension. Droplets (~6.9 nL) were generated from this sample and displayed onto APTES modified Petri dish. Sessile droplets on APTES modified surface had a slightly larger size and thinner thickness compare to those on untreated surface (Fig. S1D-E). The spherical shape of the droplets on untreated surface resulted in refraction and distortion of imaging by optical microscopes. In comparison, the APTES modified surface provides distortion-free imaging under an inverted microscope. This allowed us to obtain a higher cell count in the sessile

droplets (cell count: 23, Fig. S1E) than cell counted from the same volume droplet on untreated surface (cell count: 13, Fig. S1D) or in Teflon tubing (cell count: 11, Fig. S1C). It is notable that cells on the edge were clearly observed only in sessile droplets on the APTES modified surface.

Construction and operation of the dish drive for spiral streaking. The automated dish drive was composed of a microstepping spindle motor (Electric Rotary Actuator, Koganei, Tokyo, Japan) and a linear translation stage (Nanotec Electronic, Munich, Germany) (Fig. S2A). A 32-bit microcontroller (STM32F103, STMicroelectronics Geneva, Switzerland) with codes written in-house was used to control the spindle motor and the linear translation stage, and communicate with a laptop via USB interface. A program written in LabVIEW, setting and sending parameters to the microcontroller, to control the automated dish drive in accordance with constant linear velocity (CLV) model.

CLV model. To automatically streak droplets in closely packed spiral tracks with high capacity, the dish drive was programmed according to CLV scheme (Fig. S2B). Briefly, when the dish moved on the spiral tracks within the writing area from the inner diameter of R_1 to outer diameter of R_2, if the track spacing was set to Δr, the number of spiral tracks in the writing area was described as in (eq.1):

$$N(R_1, R_2) = \frac{R_2 - R_1}{\Delta r} \quad \text{(eq.1)}$$

The total number of droplets on the spiral tracks was the total length of tracks divided by spacing between adjacent droplets, as described in (eq.2):

$$\mathrm{n}(R_1, R_2) = \frac{\mathrm{L}(R_1, R_2)}{\Delta l} = \frac{2\pi \frac{R_1 + R_2}{2} \mathrm{N}(R_1, R_2)}{\Delta l} = \pi \frac{R_2^2 - R_1^2}{\Delta r \Delta l} \quad \text{(eq.2)}$$

As the platform was operated with a CLV of V, The velocity could be expressed as the total length of tracks $L(R_1, R_2)$ divided by the total time elapsed T, or the length of tracks $L(R_1, r)$ divided by time elapsed during a particular interval t:

$$V = \frac{L(R_1, R_2)}{T} = \frac{L(R_1, r)}{t}, \quad 0 \le t \le T \quad \text{(eq.3)}$$

Based on (eq.1) - (eq.3), the radial position at any time t could be derived as (eq.4):

$$r(t) = \sqrt{\frac{t}{t_{max}}(R_2^2 - r_1^2) + r_1^2} \quad \text{(eq.4)}$$

To operate with linear velocity of V, the rotational angular velocity (ω) of the spindle motor and the velocity of the linear translator (u) moving radially outwards could be expressed as (eq.5) and (eq.6):

$$\omega(t) = \frac{V}{r(t)} \quad \text{(eq.5)}$$

$$u(t) = \frac{dr}{dt} \quad \text{(eq.6)}$$

Depending on (eq.4) - (eq.6), we could get the rotational angular velocity (ω) and the velocity of the linear translator (u) if R_1, R_2, Δr and V are determined. The typical rotational angular velocity (ω) and the velocity of the linear translator (u) were plotted against time (Fig. S2C). Based on (eq.4), with a constant droplet generating frequency, the droplets

written on the dish could be easily addressed and indexed according to its radial position (Fig. S2D).

Fabrication and operation of droplet generating Device. There were two types of devices used in this research for microfluidic generating of mono-disperse droplets, the capillary-based device and the microfabricated PDMS device. The capillary-based device was fabricated by assembly of two 1.5-cm long fused-silica capillaries (40 μm I.D., 103 μm O.D.) with a Teflon tubing (15 to 30 cm long, 250 μm O.D., 200 μm I.D.) (Fig. S3A-B). The two capillaries were parallel inserted into the open end of the Teflon tubing and sealed with epoxy. The other end of the Teflon tubing extended to the streaking tip as described below.

PDMS devices were made by soft lithographic techniques (1) as described (2). Photolithorgraphy was performed with URE-2000/35 Mask Aligner (Institute of Optics and Electronics, Chinese Academy of Sciences, Chengdu, China). A Teflon tubing (15 to 30 cm long, 250 μm O.D., 200 μm I.D.), cut at an angle (~45°) to facilitate collecting of droplets, was inserted into the junction of the microchannels (200 μm in height, 200 μm in width) of the device through the outlet microchannel. Connections of Teflon tubing and PDMS devices were sealed with capillary wax (Hampton Research, Aliso Viejo, CA, USA).

Agilent gastight syringes with 30-gauge Teflon tubing were used to load aqueous solutions and carrier oil. Pump 11 Pico Plus elite syringe pumps controlled with LabVIEW

programs were used to drive flows. For capillary-based device, aqueous solutions and carrier oil were delivered via two fused-silica capillaries, and mono-disperse droplets were formed in the Teflon tubing. For PDMS-based device, the sample was mixed with another two aqueous reagents with constant mixing ratio or ramping programs, and co-flowed with carrier oil at the -junction to form droplets directly into the Teflon tubing (Fig. S3C).

Streaking tip fabrication and manual streaking operation. For manual streaking, 30-cm long Teflon tubing was used in the droplet generation devices. A pipette tip (200 μL size) was used as the conical sleeve surrounds the end of the Teflon tubing to reinforce the flexible Teflon tubing during manual streaking. The end of the tubing was leveled with the conical pipette tip outlet for easy streaking. For easy holding, the pipette tip was coupled with a plastic tube (5 cm in length, 3.5 mm O.D., 2 mm I.D.). To manually streak sessile droplet array, The device was connected with syringe pumps to forming droplet in the Teflon tubing, and the streaking tip was held by hand with a slightly angle (~5°) from vertical and touched the surface of Petri dish filled with mineral oil (10 mL). The streaking tip was dragged following a zig-zag pattern, with approximate line spacing of about 1.5 mm.

Tracking serial dilution using spiral droplet array. 0.5% (w/v) blue, yellow and red food dye solutions in Deionized water were used for evaluation of serial dilution in droplets.

Mineral oil was used as the carrier oil. The ramping program of flow rates was written in LabVIEW, which set the total flow rate to 3 μL/min, and ramped up or down flow rate of either blue, yellow or red dye solution to generate the rainbow color droplets. Pictures of the droplet array were taken with a compact camera (Nikon1 J1, Nikon, Tokyo, Japan) (Fig. 4D).

Determination of degradation rate of fluoranthene by isolated strains. The microbial isolates which could form transparent circles on MSM-fluoranthene agar plates and further grow on MSM-fluoranthene broth were characterized for capability of fluoranthene degradation. Three replicates were performed for each isolates. Fluoranthene in cultured samples after 9 days incubation were extracted with ethyl acetate for three times. All three extracts were pooled and concentrated by evaporation under nitrogen gas to 1 mL. Fluoranthene was quantified by a high performance liquid chromatography system (Agilent 1200 series, CA, USA) equipped with a ZORBAX Eclipse Plus C18 column (4.6 mm × 250 mm). The elute was performed by an acetonitrile-water (65:35) system at a flow rate of 1.2 mL/min and were detected at 254 nm. The degradation rate of fluoranthene was derived as (eq.7):

$$R_d = \frac{C_0 - C}{C_0} \times 100\% \qquad \text{(eq.7)}$$

where R_d (%) represents the degradation rate, C_0 (mg/L) represents the initial concentration of fluoranthene, and C (mg/L) represents the remained concentration of fluoranthene after incubation with the bacterial strain.

Metagenomic sequencing. Cells pooled from agar plates and MSPs using fluoranthene as the sole carbon source were used for metagenomic sequencing. Total DNAs were extracted with E.Z.N.A Mag-Bind Soil DNA Kit (Omega Bio-Tek, GA, USA) (3) by using a KingFisher Flex Magnetic Particle Processor (Thermo Scientific, MA, USA). Extractions were performed according to kit and instrument protocols. Eluted DNAs were used for 16S rRNA gene V4 region PCR amplification with the U515F (5'-GTGCCAGCMGCCGCGGTAA-3') and 806R (5'-GGACTACHVGGGTWTCTAAT-3') (4) primers containing barcodes at the 5' end of the front primer (5). PCR reactions were performed in 50 μL volumes, each containing 1.5 μL of 10 μM forward and reverse primers respectively, 25 μL of 2× KAPA HiFi HotStart ReadyMix (Kapa Biosystems, Inc., MA, USA), and up to 23 μL of extracted DNA as a template. The PCRs were performed as follows: 32 cycles (98 °C, 20 s; 54 °C, 15 s; 72°C, 15 s) after an initial denaturation at 95 °C for 3 min, following a final extension at 72 °C for 60 s. Triplicate PCR products for each samples were purified using E.Z.N.A. Gel Extraction Kit (Omega Bio-Tek, Inc., GA, USA) and then quantified using Qubit dsDNA HS Assay Kits (Invitrogen, CA, USA). Equal amounts of PCR products were mixed to produce equivalent sequencing depth from all

samples. After purification by using Agencourt AMPure XP KIT, the pooled-PCR products were used to construct a DNA library using NEB E7370L DNA Library Preparation Kit according to instructions from Illumina (San Diego, California, USA). Finally, the single composite barcoded PCR product was sequenced on a MiSeq machine using PE250 protocol.

Sequence data processing and statistical analysis. Paired-end Illumina generated reads were subjected to the Skewer program (version 0.1.123) (6) with an error threshold of 0.2 for adapter trimming and de-multiplexing. The trimmed paired-reads were merged by the PEAR program (version 0.9.5) (7) with *p*-value of 0.01. Sequence reads were filtered (fastq_maxee = 0.5 and fastq_trunclen = 289), removed replication and discarded singletons followed the data handling procedure of Edgar and the website (http://drive5.com/usearch/manual/uparse_cmds.html, Edgar, R., UPARSE Commands, Date of access: 19/1/2015). On average, there were more than 30,000 raw sequences of each sample obtained for downstream data analysis. Operational taxonomic units (OTUs) were clustered at 97% similarity, checked for chimeras and abundance calculated with Uparse pipeline (8). Finally, qualified sequences were analyzed for relative abundance calculation (Table S1), and α-diversity indexes analysis with QIIME (9). Coverage was calculated using the equation:

$$\mathrm{C} = (1 - \frac{n}{N}) \times 100\% \qquad \text{(eq.8)}$$

where *n* is the number of unique OTU and N is the total number of clones examined (10).

SUPPLEMENTAL REFERENCES:

1. **Duffy, D. C., J. C. McDonald, O. Schueller, and G. M. Whitesides.** 1998. Rapid prototyping of microfluidic systems in poly(dimethylsiloxane). Anal Chem **70:**4974-4984. http://dx.doi.org/10.1021/ac980656z.
2. **Chen, D., W. B. Du, Y. Liu, W. S. Liu, A. Kuznetsov, F. E. Mendez, L. H. Philipson, and R. F. Ismagilov.** 2008. The chemistrode: A droplet-based microfluidic device for stimulation and recording with high temporal, spatial, and chemical resolution. Proc Natl Acad Sci U S A **105:**16843-16848. http://dx.doi.org/10.1073/pnas.0807916105.
3. **Lau, H. K., L. M. Clotilde, A. P. Lin, G. L. Hartman, and C. R. Lauzon.** 2013. Comparison of IMS Platforms for detecting and recovering Escherichia coli O157 and Shigella flexneri in foods. J Lab Autom **18:**178-183. http://dx.doi.org/10.1177/2211068212468583.
4. **Caporaso, J. G., C. L. Lauber, W. A. Walters, D. Berg-Lyons, C. A. Lozupone, P. J. Turnbaugh, N. Fierer, and R. Knight.** 2011. Global patterns of 16S rRNA diversity at a depth of millions of sequences per sample. Proc Natl Acad Sci U S A **108 Suppl 1:**4516-4522. http://dx.doi.org/10.1073/pnas.1000080107.
5. **Bates, S. T., D. Berg-Lyons, J. G. Caporaso, W. A. Walters, R. Knight, and N. Fierer.** 2011. Examining the global distribution of dominant archaeal populations in soil. ISME J **5:**908-917. http://dx.doi.org/10.1038/ismej.2010.171.
6. **Jiang, H., R. Lei, S. W. Ding, and S. Zhu.** 2014. Skewer: a fast and accurate adapter trimmer for next-generation sequencing paired-end reads. BMC Bioinformatics **15:**182. http://dx.doi.org/10.1186/1471-2105-15-182.
7. **Zhang, J., K. Kobert, T. Flouri, and A. Stamatakis.** 2014. PEAR: a fast and accurate

Illumina Paired-End reAd mergeR. Bioinformatics **30:**614-620. http://dx.doi.org/10.1093/bioinformatics/btt593.

8. **Edgar, R. C.** 2013. UPARSE: highly accurate OTU sequences from microbial amplicon reads. Nat Methods **10:**996-998. http://dx.doi.org/10.1038/nmeth.2604.
9. **Caporaso, J. G., J. Kuczynski, J. Stombaugh, K. Bittinger, F. D. Bushman, E. K. Costello, N. Fierer, A. G. Pena, J. K. Goodrich, J. I. Gordon, G. A. Huttley, S. T. Kelley, D. Knights, J. E. Koenig, R. E. Ley, C. A. Lozupone, D. McDonald, B. D. Muegge, M. Pirrung, J. Reeder, J. R. Sevinsky, P. J. Turnbaugh, W. A. Walters, J. Widmann, T. Yatsunenko, J. Zaneveld, and R. Knight.** 2010. QIIME allows analysis of high-throughput community sequencing data. Nat Methods **7:**335-336. http://dx.doi.org/10.1038/nmeth.f.303.
10. **Ravenschlag, K., K. Sahm, J. Pernthaler, and R. Amann.** 1999. High bacterial diversity in permanently cold marine sediments. Appl Environ Microbiol **65:**3982-3989.

SUPPLEMENTAL FIGURES:

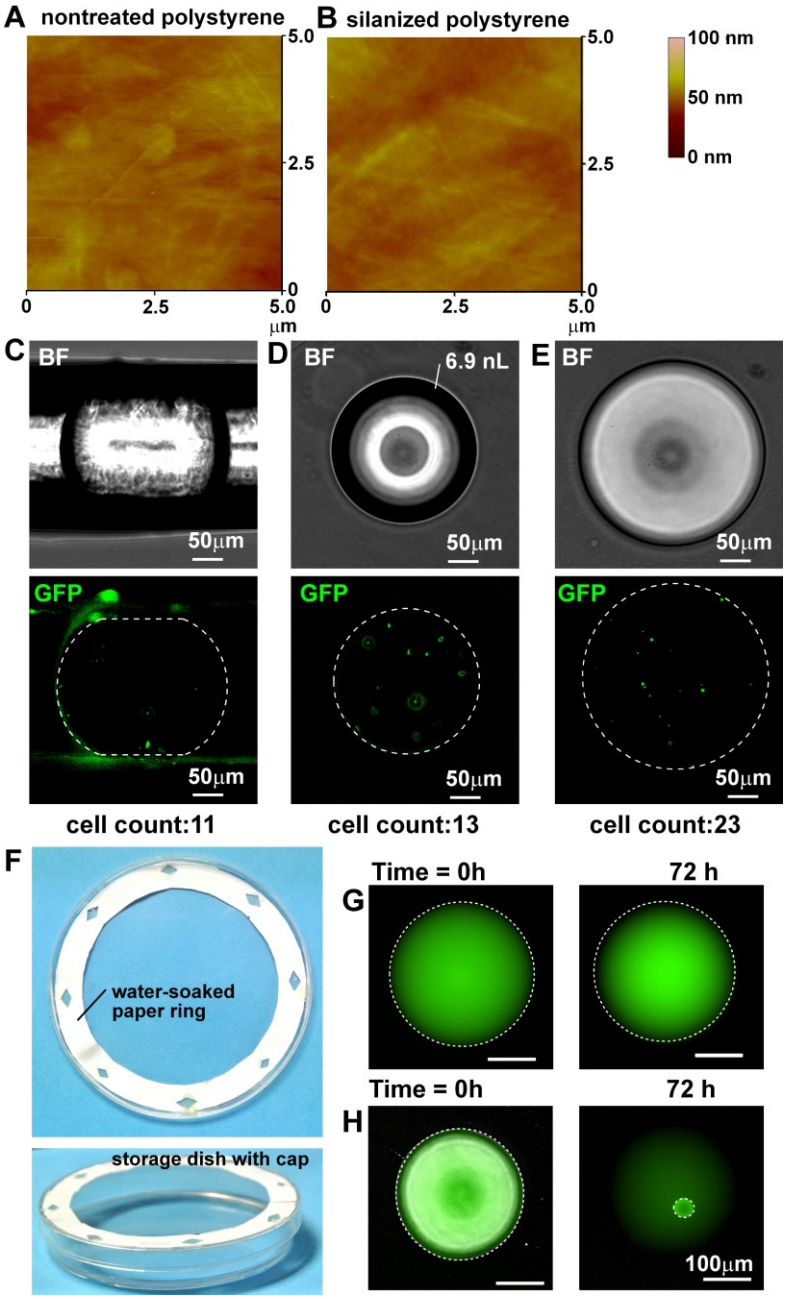

FIG S1. Modification and characterization of Polystyrene Petri dishes for droplet storage. (A-B) AFM images of untreated (A) and APTES-modified (B) surface. (C) Bright-field and green fluorescence images of 6.9 nL LB droplet containing GFP-tagged *Pseudomonas aeruginosa* PAO1 in a 200 μm I.D. Teflon tubing, on untreated Petri dish, and APTES-modified Petri dish. (D) Prevention of long-term evaporation during incubation by attaching a paper ring to the lid; Evaporation of droplets with fluorescein was monitored in 72 hours with (E) and without (F) wet paper ring.

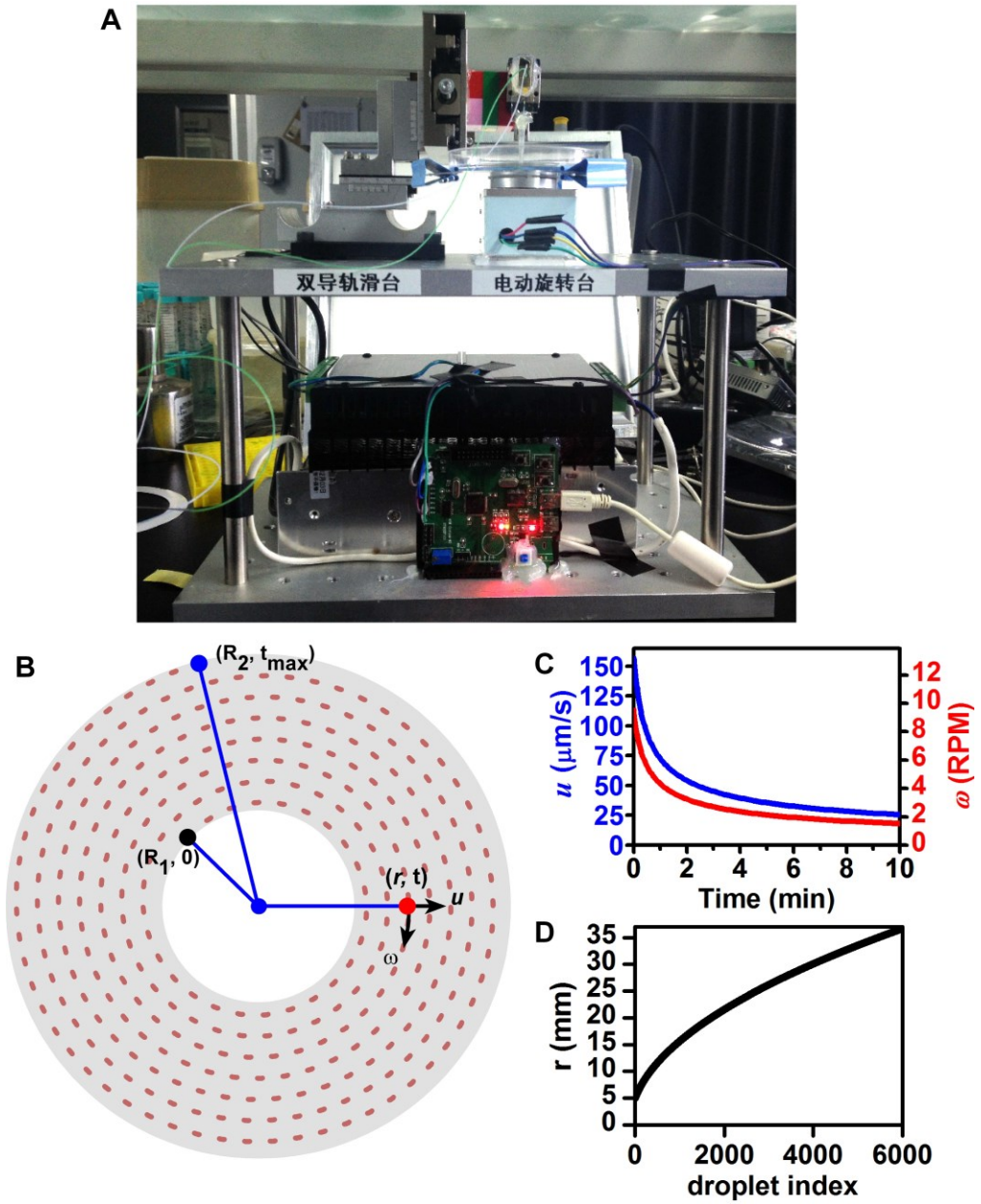

FIG S2. The constant linear velocity (CLV) model for streaking of sessile droplets on Petri dish. (A) A picture of the dish drive setup. (B) The typical spiral tracks generated by the CLV model. (C) Plots of the rotation angular velocity (ω) and the velocity of the linear translator (u) as a function of time. (D) A Plot of distance of droplets from the center as a function of the indexes of the droplets on the spiral tracks.

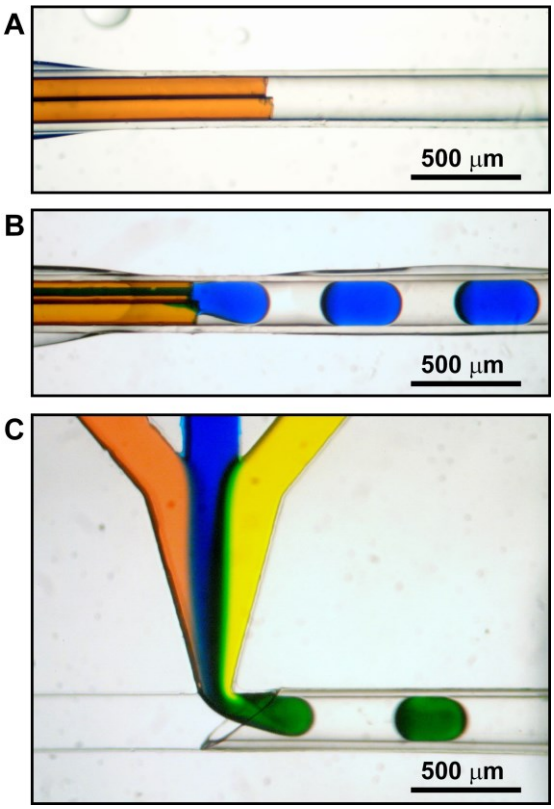

FIG S3. Microfluidic devices for forming droplets. (A) Micrograph of an empty capillary-based device with two inlets. (B) Micrograph of droplets of blue food dye solution forming directly into the Teflon tubing. (C) Micrograph of droplet formation in a four-inlet PDMS device with Teflon tubing inserted to the junction of microchannels.

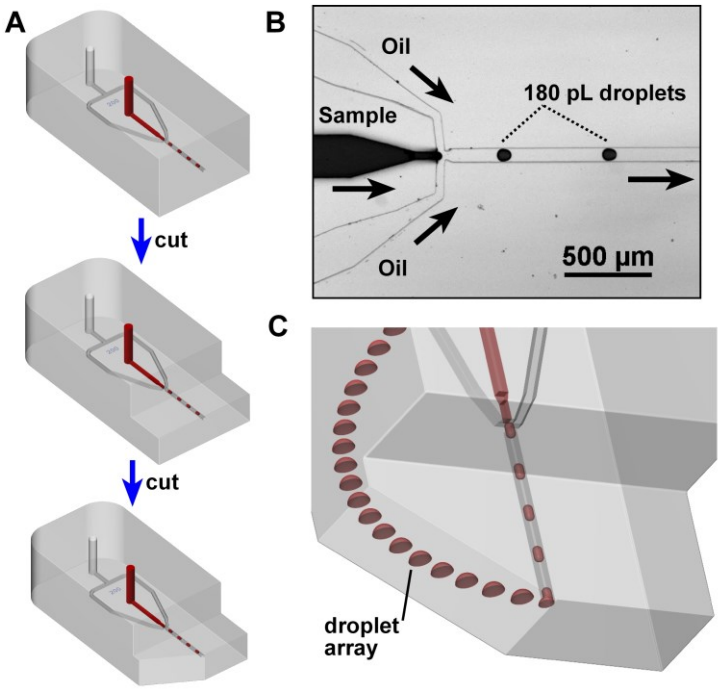

FIG S4. Fabrication of PDMS droplet-writing interface. (A) The cutting procedure of the droplet writing tip on a droplet generating device. (B) Microscopic photograph of the droplet-generation device producing 180 pL droplets. (C) 3D view from the Bottom of the writing tip during writing of droplet array on a flat transparent substrate covered by carrier oil.

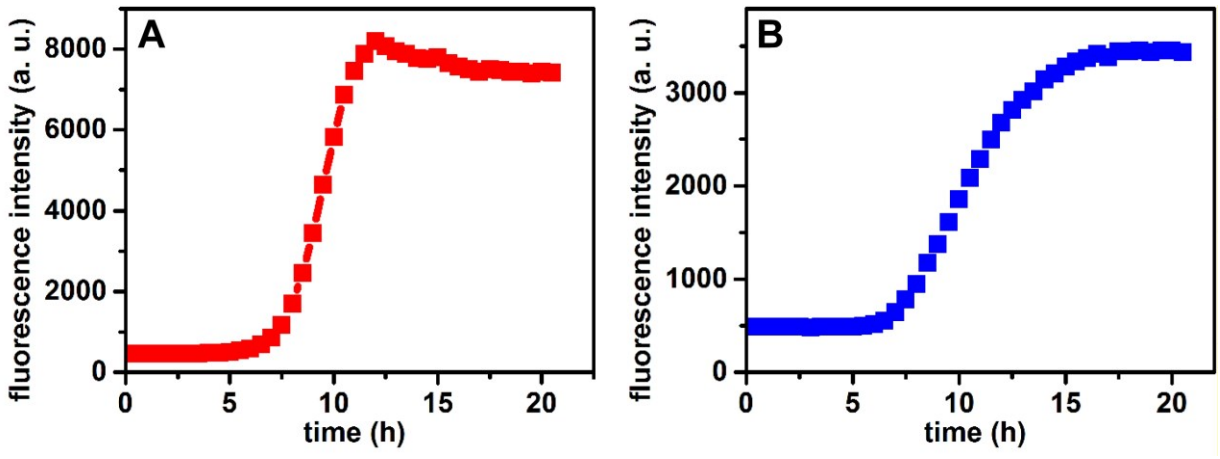

FIG S5. Typical growth curve from a single cell of RFP-tagged *E. coli* RP437 (A) and GFP-tagged *E. coli* RP1616 (B) based on integrated fluorescence intensity of droplets.

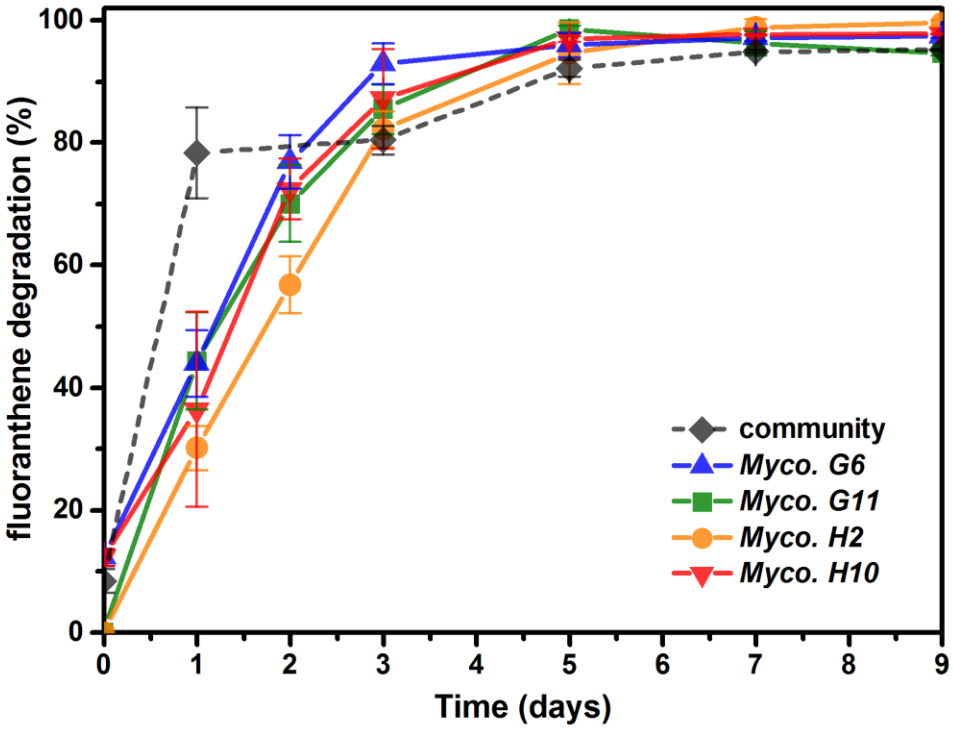

FIG S6. Efficiency of fluoranthene degradation for *Mycobacterium* strains obtained by the MSP method according to fluoranthene removal. The degradation of the original community is also plotted as the dotted gray line.

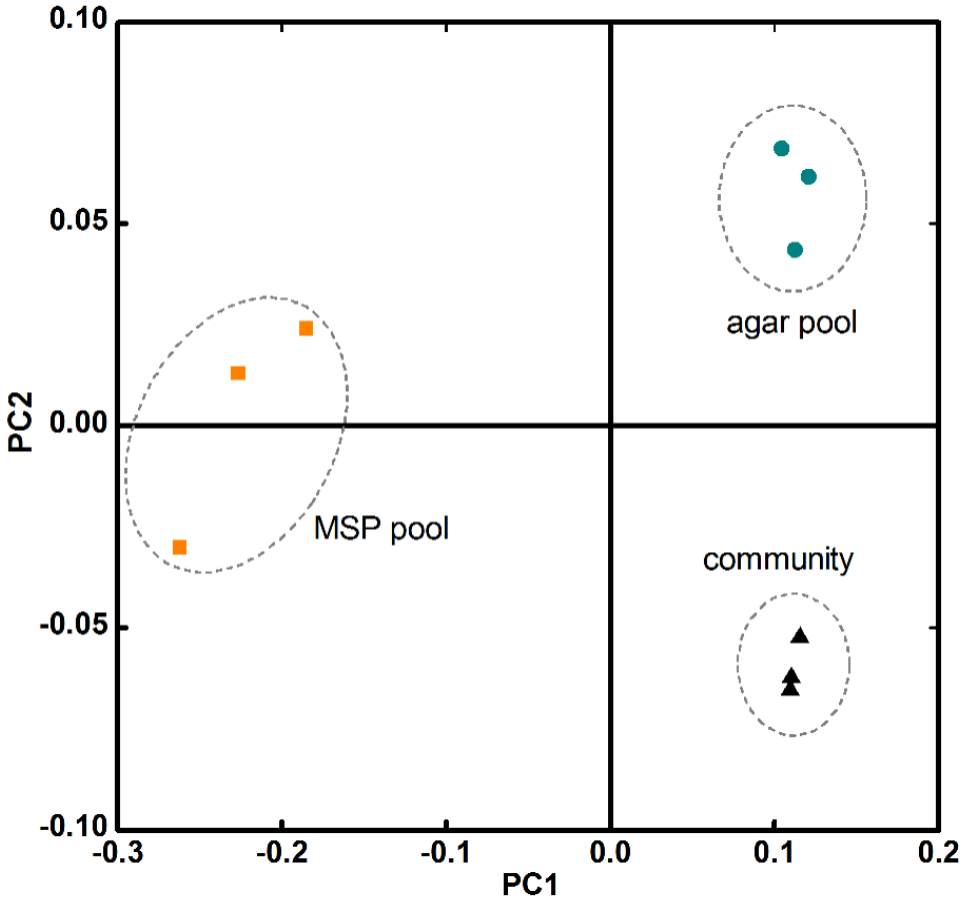

FIG S7. 2-dimentional principal coordinates analysis (PCoA) for characterizing the cluster of the three kinds of samples, including pooled cells from MSPs, pooled cells from agar plates, and the original community.

Table S1. Microbial isolates obtained from MSP method and agar plates using various culture media, and the corresponding relative abundances estimated by 16S rRNA sequencing of the original community.

Family	HTS abundance	Genus of isolates	Agar plate isolates	MSP isolates
Pseudomonadaceae	31.6659%	*Pseudomonas*	27	65
Mycobacteriaceae	20.4309%	*Mycobacterium*	0	13
Rhizobiaceae	5.4405%	*Shinella*	6	15
		Rhizobium	0	4
		Sinorhizobium	0	1
Comamonadaceae	3.7741%	*Diaphorobacter*	13	4
		Xenophilus	3	1
Xanthomonadaceae	2.3776%	*Pseudoxanthomonas*	14	4
Nocardioidaceae	1.4214%	*Nocardioides*	0	3
		Aeromicrobium	0	1
Alcaligenaceae	1.3238%	*Alcaligenes*	1	1
		Achromobacter	4	0
		Castellaniella	0	2
Sphingomonadaceae	0.3385%	*Sphingomonas*	13	1
Micrococcaceae	0.2315%	*Micrococcus*	1	14
		Kocuria	4	8
		Arthrobacter	1	4
Bradyrhizobiaceae	0.1599%	*Bosea*	0	1
		Nitrobacter	0	2
Microbacteriaceae	0.1505%	*Agrococcus*	0	1
		Curtobacterium	1	1
		Microbacterium	5	16
Enterobacteriaceae	0.1256%	*Proteus*	0	1
Moraxellaceae	0.0748%	*Acinetobacter*	4	4
		Moraxella	0	4
Planococcaceae	0.0208%	*Planomicrobium*	0	2
		Sporosarcina	0	1
		Planococcus	1	0
Flavobacteriaceae	0.0083%	*Flavobacterium*	1	0
		Myroides	0	1
Bacillaceae	0.0031%	*Bacillus*	0	8
		Lysinibacillus	0	1
		Oceanobacillus	0	2

Aerococcaceae	0.001%	*Aerococcus*	0	1
		Facklamia	0	1
Streptomycetaceae	0	*Streptomyces*	0	5
Staphylococcaceae	0	*Staphylococcus*	5	11
Pseudonocardiaceae	0	*Saccharothrix*	0	2
Paenibacillaceae	0	*Paenibacillus*	0	2
Brucellaceae	0	*Ochrobactrum*	0	1
Actinomycetales	0	*Gordonia*	0	1
Dietziaceae	0	*Dietzia*	0	1
Corynebacteriaceae	0	*Corynebacterium*	0	2
Dermabacteraceae	0	*Brachybacterium*	0	2
		Dermabacter	0	1
Nocardiaceae	0	*Rhodococcus*	1	1
Geodermatophilaceae	0	*Blastococcus*	0	1
Count of OTUs	/	47	18	44
Count of isolates			105	218

Table S2. Community profiling based on metagenomic sequencing of bacterial 16S rRNA genes. Average OTU abundances of three duplicates were given for original community, pooled cells from MSPs and pooled cells from agar plates. Fluoranthene was used as the sole carbon source.

Taxon	community	MSP pooled	agar plate pooled
Unassigned;Other;Other;Other;Other;Other	0.00435	0.003426	0.003977
p__Acidobacteria;c__Acidobacteriia;o__Acidobacteriales;f__Acidobacteriaceae;g__	0	0	3.11E-05
p__Acidobacteria;c__Solibacteres;o__Solibacterales;f__Solibacteraceae;g__	3.11E-05	0	4.15E-05
p__Acidobacteria;c__[Chloracidobacteria];o__RB41;f__Ellin6075;g__	3.11E-05	0	0.000104
p__Actinobacteria;c__Actinobacteria;o__Actinomycetales;f__Frankiaceae;g__	0.000166	0.000488	0.00053
p__Actinobacteria;c__Actinobacteria;o__Actinomycetales;f__Intrasporangiaceae;g__Knoellia	0	5.19E-05	0
p__Actinobacteria;c__Actinobacteria;o__Actinomycetales;f__Intrasporangiaceae;g__Phycicoccus	0	4.17E-05	0
p__Actinobacteria;c__Actinobacteria;o__Actinomycetales;f__Microbacteriaceae;g__	4.15E-05	2.08E-05	9.37E-05
p__Actinobacteria;c__Actinobacteria;o__Actinomycetales;f__Microbacteriaceae;g__Microbacterium	0.001464	0.057873	0.002595

p__Actinobacteria;c__Actinobacteria;o__Actinomycetales;f__Micrococcaceae;Other	0.001163	0.003893	0.005201
p__Actinobacteria;c__Actinobacteria;o__Actinomycetales;f__Micrococcaceae;g__	0.001153	0.003021	0.005326
p__Actinobacteria;c__Actinobacteria;o__Actinomycetales;f__Micrococcaceae;g__Microbispora	0	7.26E-05	0
p__Actinobacteria;c__Actinobacteria;o__Actinomycetales;f__Mycobacteriaceae;g__Mycobacterium	0.204309	0.012646	0.067206
p__Actinobacteria;c__Actinobacteria;o__Actinomycetales;f__Nocardioidaceae;g__	0.014214	0.001173	0.004859
p__Actinobacteria;c__Actinobacteria;o__Actinomycetales;f__Propionibacteriaceae;g__Propionibacterium	3.11E-05	0.000488	2.07E-05
p__Actinobacteria;c__Thermoleophilia;o__Gaiellales;f__;g__	0.000197	1.04E-05	0.000145
p__Bacteroidetes;c__Bacteroidia;o__Bacteroidales;f__Bacteroidaceae;g__Bacteroides	1.04E-05	0.000426	0
p__Bacteroidetes;c__Bacteroidia;o__Bacteroidales;f__ML635J-40;g__	0	2.07E-05	0
p__Bacteroidetes;c__Flavobacteriia;o__Flavobacteriales;f__Flavobacteriaceae;g__Flavobacterium	2.07E-05	0.001568	2.08E-05
p__Bacteroidetes;c__Flavobacteriia;o__Flavobacteriales;f__Flavobacteriaceae;g__Myroides	6.23E-05	0.002886	2.08E-05
p__Bacteroidetes;c__Flavobacteriia;o__Flavobacteriales;f__[Weeksellaceae];g__Chryseobacterium	0.0152	0.001256	0.001817
p__Bacteroidetes;c__Flavobacteriia;o__Flavobacteriales;f__[Weeksellaceae];g__Wautersiella	0	8.3E-05	0
p__Bacteroidetes;c__Sphingobacteriia;o__Sphingobacteriales;f__;g__	1.04E-05	0.000249	1.04E-05
p__Bacteroidetes;c__Sphingobacteriia;o__Sphingobacteriales;f__Sphingobacteriaceae;g__	0.006811	0.000343	0.000478
p__Bacteroidetes;c__Sphingobacteriia;o__Sphingobacteriales;f__Sphingobacteriaceae;g__Sphingobacterium	1.04E-05	0.000156	0
p__Bacteroidetes;c__[Saprospirae];o__[Saprospirales];f__Chitinophagaceae;g__	0.00081	0.000197	0.003291
p__Bacteroidetes;c__[Saprospirae];o__[Saprospirales];f__Chitinophagaceae;g__Chitinophaga	0.000291	0.000737	0.012189
p__Chloroflexi;c__Anaerolineae;o__Anaerolineales;f__Anaerolinaceae;g__T78	0	6.24E-05	0
p__Chloroflexi;c__Anaerolineae;o__envOPS12;f__;g__	0	1.04E-05	0
p__Cyanobacteria;c__Chloroplast;o__Streptophyta;f__;g__	0	6.24E-05	0
p__Firmicutes;c__Bacilli;o__Bacillales;f__Alicyclobacillaceae;g__	1.04E-05	0	2.08E-05
p__Firmicutes;c__Bacilli;o__Bacillales;f__Bacillaceae;g__Bacillus	3.11E-05	0.000125	0.000145
p__Firmicutes;c__Bacilli;o__Bacillales;f__Listeriaceae;g__Brochothrix	0.000301	0.013092	0.000426
p__Firmicutes;c__Bacilli;o__Bacillales;f__Planococcaceae;Other	9.36E-05	0.000104	0.000332

p__Firmicutes;c__Bacilli;o__Bacillales;f__Planococcaceae;g__Planococcus	7.26E-05	0.000208	8.32E-05
p__Firmicutes;c__Bacilli;o__Bacillales;f__Planococcaceae;g__Sporosarcina	4.15E-05	4.15E-05	0.000104
p__Firmicutes;c__Bacilli;o__Bacillales;f__Staphylococcaceae;g__Staphylococcus	0	0.000207	2.08E-05
p__Firmicutes;c__Bacilli;o__Lactobacillales;f__Aerococcaceae;g__	0	3.11E-05	0
p__Firmicutes;c__Bacilli;o__Lactobacillales;f__Aerococcaceae;g__Facklamia	1.04E-05	0.000187	0
p__Firmicutes;c__Bacilli;o__Lactobacillales;f__Carnobacteriaceae;g__Carnobacterium	0.000239	0.005929	0.000228
p__Firmicutes;c__Bacilli;o__Lactobacillales;f__Enterococcaceae;g__Enterococcus	0.001018	0.001941	0.002159
p__Firmicutes;c__Bacilli;o__Lactobacillales;f__Lactobacillaceae;g__Lactobacillus	4.15E-05	0.001433	4.15E-05
p__Firmicutes;c__Bacilli;o__Lactobacillales;f__Leuconostocaceae;g__Leuconostoc	0.000239	0.012542	0.000249
p__Firmicutes;c__Bacilli;o__Lactobacillales;f__Streptococcaceae;g__Lactococcus	0.01222	0.556622	0.008981
p__Firmicutes;c__Bacilli;o__Lactobacillales;f__Streptococcaceae;g__Streptococcus	0.000405	0.015771	0.000301
p__Firmicutes;c__Clostridia;o__Clostridiales;f__;g__	0	3.11E-05	0
p__Firmicutes;c__Clostridia;o__Clostridiales;f__Peptococcaceae;g__Desulfosporosinus	9.35E-05	0.000197	6.24E-05
p__Firmicutes;c__Clostridia;o__Clostridiales;f__[Mogibacteriaceae];g__Mogibacterium	1.04E-05	3.11E-05	1.04E-05
p__Firmicutes;c__Clostridia;o__Clostridiales;f__[Tissierellaceae];g__Finegoldia	0	1.04E-05	0
p__Firmicutes;c__Clostridia;o__Clostridiales;f__[Tissierellaceae];g__Helcococcus	0	4.15E-05	0
p__Firmicutes;c__Clostridia;o__Clostridiales;f__[Tissierellaceae];g__Peptoniphilus	1.04E-05	1.04E-05	0
p__Firmicutes;c__Clostridia;o__Clostridiales;f__[Tissierellaceae];g__Tissierella_Soehngenia	1.04E-05	0.000343	1.04E-05
p__Fusobacteria;c__Fusobacteriia;o__Fusobacteriales;f__Fusobacteriaceae;g__Fusobacterium	0	7.28E-05	0
p__Planctomycetes;c__OM190;o__CL500-15;f__;g__	0	1.04E-05	0
p__Planctomycetes;c__Planctomycetia;o__Gemmatales;f__Isosphaeraceae;g__	0.000322	4.15E-05	0.000758
p__Proteobacteria;c__Alphaproteobacteria;o__Caulobacterales;f__Caulobacteraceae;g__	0.010258	0.001952	0.006852
p__Proteobacteria;c__Alphaproteobacteria;o__Caulobacterales;f__Caulobacteraceae;g__Phenylobacterium	0.000519	3.11E-05	0.000291
p__Proteobacteria;c__Alphaproteobacteria;o__Rhizobiales;Other;Other	5.2E-05	0.000997	7.28E-05
p__Proteobacteria;c__Alphaproteobacteria;o__Rhizobiales;f__;g__	0.001101	0.000197	0.000426

p__Proteobacteria;c__Alphaproteobacteria;o__Rhizobiales;f__Bradyrhizobiaceae;Other	0.000841	0.006645	0.000862
p__Proteobacteria;c__Alphaproteobacteria;o__Rhizobiales;f__Bradyrhizobiaceae;g__	0.000758	0.007247	0.000903
p__Proteobacteria;c__Alphaproteobacteria;o__Rhizobiales;f__Hyphomicrobiaceae;Other	0.000177	0.000145	0.000197
p__Proteobacteria;c__Alphaproteobacteria;o__Rhizobiales;f__Hyphomicrobiaceae;g__Devosia	0.000207	4.15E-05	0.000384
p__Proteobacteria;c__Alphaproteobacteria;o__Rhizobiales;f__Hyphomicrobiaceae;g__Hyphomicrobium	0.009303	0.001132	0.005534
p__Proteobacteria;c__Alphaproteobacteria;o__Rhizobiales;f__Methylobacteriaceae;g__	0	2.07E-05	0
p__Proteobacteria;c__Alphaproteobacteria;o__Rhizobiales;f__Methylobacteriaceae;g__Methylobacterium	4.15E-05	0.000425	2.07E-05
p__Proteobacteria;c__Alphaproteobacteria;o__Rhizobiales;f__Phyllobacteriaceae;g__Aminobacter	0.000187	7.27E-05	2.07E-05
p__Proteobacteria;c__Alphaproteobacteria;o__Rhizobiales;f__Rhizobiaceae;g__	0.006967	0.001111	0.003447
p__Proteobacteria;c__Alphaproteobacteria;o__Rhizobiales;f__Rhizobiaceae;g__Agrobacterium	0.047438	0.006126	0.025728
p__Proteobacteria;c__Alphaproteobacteria;o__Rhizobiales;f__Xanthobacteraceae;Other	3.11E-05	2.07E-05	1.04E-05
p__Proteobacteria;c__Alphaproteobacteria;o__Rhodobacterales;f__Rhodobacteraceae;g__	1.04E-05	4.17E-05	0
p__Proteobacteria;c__Alphaproteobacteria;o__Rhodobacterales;f__Rhodobacteraceae;g__Paracoccus	3.11E-05	0.000737	6.24E-05
p__Proteobacteria;c__Alphaproteobacteria;o__Rhodospirillales;f__Rhodospirillaceae;g__	0.004247	0.00054	0.002305
p__Proteobacteria;c__Alphaproteobacteria;o__Rhodospirillales;f__Rhodospirillaceae;g__Magnetospirillum	0.000259	1.04E-05	9.35E-05
p__Proteobacteria;c__Alphaproteobacteria;o__Rhodospirillales;f__Rhodospirillaceae;g__Phaeospirillum	0.000987	9.37E-05	0.00026
p__Proteobacteria;c__Alphaproteobacteria;o__Sphingomonadales;f__Sphingomonadaceae;Other	0.000114	1.04E-05	2.08E-05
p__Proteobacteria;c__Alphaproteobacteria;o__Sphingomonadales;f__Sphingomonadaceae;g__Sphingobium	5.19E-05	0.000218	0.000145
p__Proteobacteria;c__Alphaproteobacteria;o__Sphingomonadales;f__Sphingomonadaceae;g__Sphingomonas	0.000716	0.003447	0.001495
p__Proteobacteria;c__Alphaproteobacteria;o__Sphingomonadales;f__Sphingomonadaceae;g__Sphingopyxis	0.002502	0.005679	0.059129

p__Proteobacteria;c__Betaproteobacteria;o__;f__;g__	0.000851	0.000135	0.00026
p__Proteobacteria;c__Betaproteobacteria;o__Burkholderiales;f__Alcaligenaceae;g__	0.005275	0.001392	0.006562
p__Proteobacteria;c__Betaproteobacteria;o__Burkholderiales;f__Alcaligenaceae;g__Achromobacter	0.004786	0.001422	0.005939
p__Proteobacteria;c__Betaproteobacteria;o__Burkholderiales;f__Alcaligenaceae;g__Denitrobacter	0.000363	9.35E-05	0.000145
p__Proteobacteria;c__Betaproteobacteria;o__Burkholderiales;f__Alcaligenaceae;g__Pigmentiphaga	0.002813	0.000197	0.00163
p__Proteobacteria;c__Betaproteobacteria;o__Burkholderiales;f__Burkholderiaceae;g__Burkholderia	0.000737	0.005181	0.000768
p__Proteobacteria;c__Betaproteobacteria;o__Burkholderiales;f__Comamonadaceae;Other	0.019249	0.009427	0.016602
p__Proteobacteria;c__Betaproteobacteria;o__Burkholderiales;f__Comamonadaceae;g__	0.003717	0.001973	0.002367
p__Proteobacteria;c__Betaproteobacteria;o__Burkholderiales;f__Comamonadaceae;g__Diaphorobacter	0.009012	0.005493	0.011203
p__Proteobacteria;c__Betaproteobacteria;o__Burkholderiales;f__Comamonadaceae;g__Hylemonella	0.005763	0.00055	0.002928
p__Proteobacteria;c__Betaproteobacteria;o__Burkholderiales;f__Oxalobacteraceae;Other	0.000529	7.28E-05	6.24E-05
p__Proteobacteria;c__Betaproteobacteria;o__Burkholderiales;f__Oxalobacteraceae;g__	2.07E-05	0.000498	0
p__Proteobacteria;c__Betaproteobacteria;o__Burkholderiales;f__Oxalobacteraceae;g__Janthinobacterium	2.07E-05	0.001204	0.000124
p__Proteobacteria;c__Betaproteobacteria;o__Burkholderiales;f__Oxalobacteraceae;g__Ralstonia	5.19E-05	0.000312	5.19E-05
p__Proteobacteria;c__Betaproteobacteria;o__Neisseriales;f__Neisseriaceae;g__	1.04E-05	0.000831	1.04E-05
p__Proteobacteria;c__Betaproteobacteria;o__Rhodocyclales;f__Rhodocyclaceae;g__	5.2E-05	0.000436	3.11E-05
p__Proteobacteria;c__Gammaproteobacteria;o__Enterobacteriales;f__Enterobacteriaceae;g__	0.001256	0.008981	0.000831
p__Proteobacteria;c__Gammaproteobacteria;o__PYR10d3;f__;g__	0.000727	9.36E-05	0.000249
p__Proteobacteria;c__Gammaproteobacteria;o__Pseudomonadales;Other;Other	**0.250283**	**0.052131**	**0.226237**
p__Proteobacteria;c__Gammaproteobacteria;o__Pseudomonadales;f__Moraxellaceae;g__	0.00028	0.008078	0.000176
p__Proteobacteria;c__Gammaproteobacteria;o__Pseudomonadales;f__Moraxellaceae;g__Acinetobacter	0.000176	0.004849	0.000156

p__Proteobacteria;c__Gammaproteobacteria;o__Pseudomonadales;f__Moraxellaceae;g__Enhydrobacter	0.000166	0.010902	0.000177
p__Proteobacteria;c__Gammaproteobacteria;o__Pseudomonadales;f__Moraxellaceae;g__Psychrobacter	0.000125	0.003115	8.32E-05
p__Proteobacteria;c__Gammaproteobacteria;o__Pseudomonadales;f__Pseudomonadaceae;Other	0.002056	0.021419	0.00136
p__Proteobacteria;c__Gammaproteobacteria;o__Pseudomonadales;f__Pseudomonadaceae;g__	0.311841	0.05969	0.269781
p__Proteobacteria;c__Gammaproteobacteria;o__Pseudomonadales;f__Pseudomonadaceae;g__Pseudomonas	0.002762	0.0285	0.001973
p__Proteobacteria;c__Gammaproteobacteria;o__Xanthomonadales;f__Sinobacteraceae;g__	0.000104	8.32E-05	5.2E-05
p__Proteobacteria;c__Gammaproteobacteria;o__Xanthomonadales;f__Sinobacteraceae;g__Nevskia	0.000851	0.01167	0.001609
p__Proteobacteria;c__Gammaproteobacteria;o__Xanthomonadales;f__Xanthomonadaceae;Other	0	0.000249	0
p__Proteobacteria;c__Gammaproteobacteria;o__Xanthomonadales;f__Xanthomonadaceae;g__Lysobacter	0	0.000239	0
p__Proteobacteria;c__Gammaproteobacteria;o__Xanthomonadales;f__Xanthomonadaceae;g__Pseudoxanthomonas	0.021056	0.023278	0.218014
p__Proteobacteria;c__Gammaproteobacteria;o__Xanthomonadales;f__Xanthomonadaceae;g__Thermomonas	0.00272	0.00028	0.000467